Partitioning of Inert Colloids Particles in Phase-Separated Polymer Solutions and their interfacial behaviour on phase boundaries

Shujie Liu

Submitted in accordance with the requirements for the degree of Master by Research

The University of Leeds

School of Food Science and Nutrition

October, 2019

The candidate confirms that the work submitted is her own, and that appropriate credit has been given where reference has been made to the work of others.

Acknowledgements

Firtsly, I would send my sincerely gratitude to Dr Rammile Ettelaie, my main supervisor, who provided me tremendous support and helped me explore the world of colloids and polymers. Thanks to your patient guidance and carefully correction, this thesis can be finished finally. Your impressive encouragement and the warm greeting every time when I meet you contribute to my confidence and optimism to my project and life here. Great thanks again. Also, I would like to thank Prof Murray, my second supervisor, who gave me many useful and inspiring advice on experimental part in the project. Your kind smiles are so sweet. Of course, I would like to thank Jianshe Chen, I would not have the chance to come to University of Leeds to begin my Master project without you.

The technicians in Food Colloids Lab 2.06, Dr Nataricha Phisarnchananan and Neil Rigby, thanks for offering training for facilities applied in my project to me. The colleges in Lab 2.06, Yue Ding, Mingduo Mu, Shuning Zhang and Xin Li, it is all of your thoughtful concern and warm heart to make my days in laboratory delightful and interesting. Also, I am grateful to Cuizhen Chen and Chenxi Hu, who helped me a lot mentally this year, it is very nice to meet you here. In the last but not the least, thank my familiy and all of my friends, you loving encouragement always cheers me up.

I would also acknowledge Zhejiang Gongshang University, my home university, which gave me this great chance to study and research in Leeds. I would never forget this tremendous journey.

Abstract

Phase separation commonly occurs in solutions containing two different incompatible polymers due to insufficient interdroplet repulsion forces and thus their coalescence. Segregative phase separation is the main type in this study, depending on the concentration when there's no specific interaction between components in analysed solution system. Introducing particles is considered to be a effective way to stabilize this unstable emulsion system.

The work focuses on the phenomenon that added inert small particles show a strong tendency to congregate into one but not the other of two phases in phase separated polymer solution system. A number of previous experimental studies by different groups indicates the wide general existence of this phenomenon. Computer simulation program is utilized here to simulate and calculate distribution of particles into each phase; using simplified model. We use the Flory-Huggins theory and Self-Consistent-Field (SCF) calculations to imitate the phase separation situation and obtain the free energy per unit area (i.e., interfacial tension) resulting from the depletion of polymers around particles in two phases to figure out whether the difference in this free energy between two phases is sufficient to induce particles to partition completely into a single phase. Self-Consistent-Field calculations, often implemented on a lattice model, allow for the variation in the volume fraction of each polymer present in a phase, to be monitored as a function of distance away from a solid interface. Indeed we find this to be the case with a strong preference for inert particles to reside in the phase enriched with smaller polymers. Several more cases for changing degree of incompatibility of two polymers, size of polymers, initial proportion of polymers are explored and discussed. In addition, the contact angle θ produced by introduced particles and the interface between two phases is approaching 90° as long as the degree of incompatibility is sufficiently large.

Experiment of observing the tendency of added fluorescent particles (Carboxyl-modified polystyrene P(S/V-COOH), Surf Green) in phase-separated solution containing κ-carrageenen and konjac gum has been done in this study. We have made phase diagram for concentration ranging from

0.1 wt% to 1.0 wt% for two polysaccharides. The result shows mixture made of higher concentrations of two solutions are prone to phase separate. And the introduced fluorescent particles observed by confocal microscopy prefers to aggregate into the phase enriched with κ-carrageenen, the smaller polysaccharide. This result just verifies the theoretical deduction to some extent.

Contents

Figure Content

Chapter 1
Introduction

1.1 Aim

When two immiscible aqueous solutions containing different water-soluble molecules are mixed to form a colloidal dispersion system with sufficient kinetic stability, this is termed a water-in-water emulsion. The two groups of molecules in the solutions interact unfavourably with each other and are therefore incompatible in solution. Water-in-water emulsion, often composed of two polymers and solvent molecules, are thought to offer great potential in the chemical, cosmetics, pharmaceuticals and food industry. Especially in the food product, where full phase separation may cause undesirable sensory properties.

However, Phase separation occurs commonly in the above system due to insufficient interdroplet repulsion forces and thus their coalescence. Segregative phase separation and associative phase separation are two major varieties. Segregative phase separation (Esquena, 2016) is the one considered in this work since it is mainly induced by repulsive interaction between polymer molecules. This instability phenomenon has been studied in a great deal of work and discovering new methods to control or adjust the stabilisation of emulsions remains an area of great importance. Addition of stabilising particles has been recognised as one effective way of preventing coalescence of droplets in recent years. A lot of studies have been done to prove and understand the function of added particles for enhancing the stability. These particles are adsorbed on the water-water interface to inhibit further phase separation.

Meanwhile, there is an interesting phenomenon discovered in many relevant experimental work (Nicolai et al., 2017) (Peddireddy et al., 2016) (Firoozmand et al., 2009) that small amount of excess nonadsorbed particles, remaining in the bulk solution, distribute themselves dominantly into one of the phases in the system irrespective of how or which polymer solution they are introduced from before the two solutions are mixed. Different methods of adding particles always result in the same situation. It is reasonable to suspect that a certain interaction exists between particles and one variety of polymer molecules to attract particles to favourably partition to one of the phases in the solution. Nevertheless, the phenomenon of fractionation still occurs when various approaches have been taken to minimise and prevent the interaction between particles and all polymers contained in the system. Therefore, scientists provide the suggestion that the phenomenon is thermodynamic driven, but with an appropriate theoretical explanation for still largely lacking.

In experimental part of the present work, two hydrocolloids, Konjac gum and kappa-carrageenan, are chosen to act as two types of incompatible polymers in solution, with the introduced particles being the fluorescent latex particles. By mixing two kinds of polymer solutions at various concentrations, the phase separation phenomenon has been observed in a range of concentration groups. Furthermore, introducing fluorescent latex particles into one polymer solution and then mixing the two polymer solutions, the added particles are seen to preferentially disperse into the phases enriched with kappa-carrageenan as expected. The results provide a partial proof of the theoretical predictions.

1.2 Phase separation of Polymer solutions

Phase separated polymer solution systems consist of at least two distinct aqueous solutions containing various polymers and solvent molecules. As a macromolecule, the polymer chains can be branched, with several types of arms, where every arm in principle is composed of different kinds of

monomers. It is widely used in the production of fibre, glue and other manufacturing fields. The choice of polymer material can be different. Most common biopolymers are protein and polysaccharides, with the latter being the choice of the polymer in our solution. Properties of solutions containing these polymers are investigated in considerable details (Grinberg et al., 1997) (Chun et al., 2014)) (Chung et al., 2013) (Pai et al., 2002).

The mixture formed by blending at least two aqueous solution containing hydrophilic polymers, when in form of droplet of one phase in the other, is also termed W/W emulsions. The stability of W/W emulsion is profoundly weak, and the solution system is prone to become fully phase separated. The incentive for phase separation of the mixed polymer solution can be diverse. There are many different interactions potentially operating in polymer solutions — hydrophobic interactions, hydrogen bonds and so on. However, compared to the electrostatic interactions, all of the above interactions are extraordinarily weak. Two types of phase separation are mostly involved in such polymer solutions, termed segregative phase separation and associative phase separation. It is well established that the occurrence of segregative phase separation and associative phase separation depends mainly on pH, ionic strength and temperature (Piculell et al., 1992) (Alves et al., 1999). Amongst these three influencing factors, pH affects the electronic charge properties of polymers. A solution system with higher charged polymers is more prone to phase separation. Ionic strength impacts on repulsive interactions between components in solution and different temperature produce solution system with various properties of intermolecular circumstance. All of the above factors contribute to the attractive or repulsive effect between the two groups of polymers, and their net effect can lead to phase separation. Segregative phase separation arises mainly in a solution containing two hydrophilic and nonionic polymers due to the negative entropy of mixing. In this case, two phases are produced, and each kind of polymer tends to reside in one of the phases. However, the concentration of molecules ought to be sufficiently high to induce phase separation. Experimental observations indicate that the same solution system would not phase-separate when the minimum sufficient concentrations of the two polymers is

not present. The solution remains a single homogenous phase, and two types of polymer molecules distribute evenly in the mixture. To illustrate an example of mixtures of proteins and polysaccharides, showing different phase situations are shown in Figure 1.2.1(Matalanis et al., 2011).

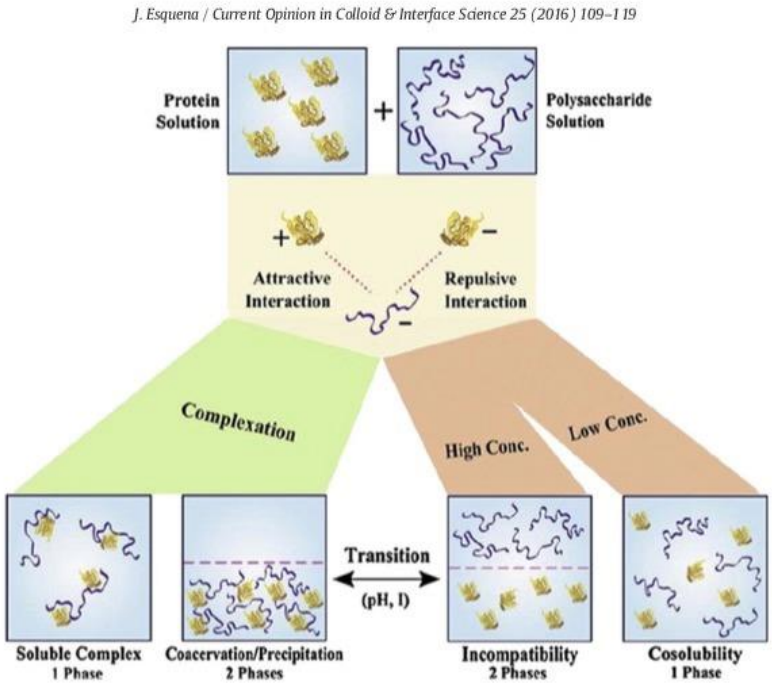

Figure 1.2.1 Four different phase separated situations that can result in mixtures of proteins and polysaccharides (Matalanis et al., 2011).

In contrast, associative phase separation is always generated in the solution system due to the oppositely charged molecules as shown in Figure 1.2.1. These molecules combine mutually to form complexes, and most of them congregate into one phase or precipitate, leaving the upper phase consisting only of solvent molecules and a few residual polymer molecules. Surprisingly, the transition between the two-phase separation types is possible when taking advantage of pH adjustment. For the different initial proportion of two polymers, the distinct consequence of final components composition of water/gelatin/maltodextrin system is shown in the phase diagram in Figure 1.2.2. The type of polymer which is dominant in volume fraction would be the continuous phase, and the other is trapped as individual domains in this continuous phase. Moreover, the phenomenon of the bicontinuous system

and phase inversion occurs when two polymers have the same volume fraction. Notably, the region beyond the binodal solid curve, also the boundary line, indicates that solution remains a single homogenous phase in these range of compositions. In contrast, when the system composition corresponds to the situation inside the binodal curve, two phases appear. The straight tie-lines, seen in Figure 1.2.2, are of great importance since they imply that any composition on a given tie-line separates into two coexisting phases with the compositions at the two extremes of each tie-line. The dashed line marks the boundary of spinodal regime. It is the region with which any small local fluctuations in concentration will grow with time, ultimately leading to the two separated phases. The boundary is characterized by the second derivative of free energy with respect to concentration, becoming zero. In contrast in the binodal regime (that between the solid and dashed lines) small density fluctuations lead to an increase in the free energy of the system and therefore will tend to disappear with time. This indicates the existence of an energy barrier which needs to be overcome before phase separation can take place. Only when a sufficiently large (and more rare) fluctuations happens to occur this can grow. This is normally associated with the requirement for the appearance of a critical nucleus size, before phase separation can proceed. The critical point is the point of shortest tie-line, where two immiscible phases gradually vanish and terminated into a single phase (Esquena, 2016).

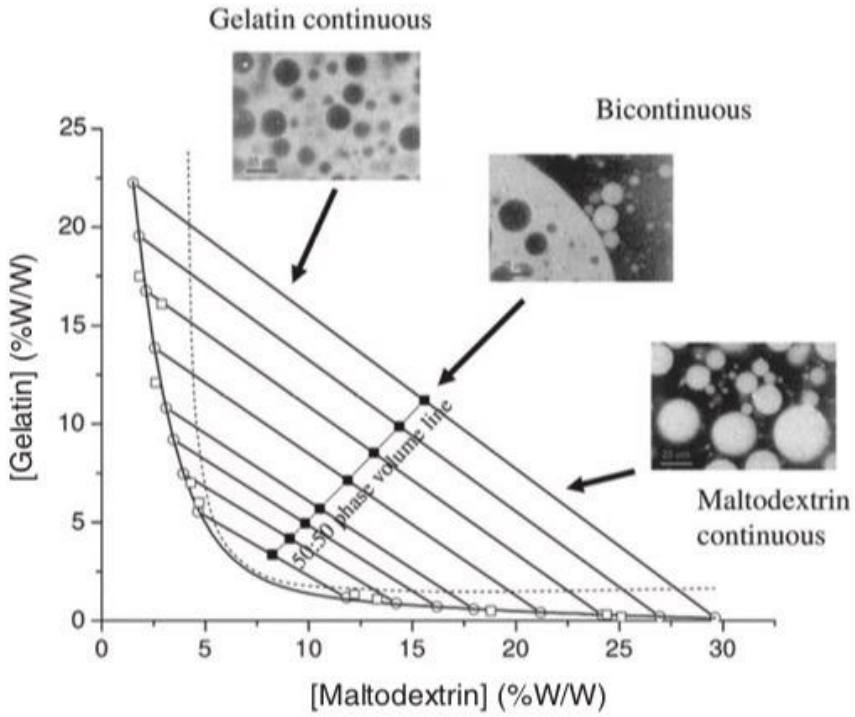

Figure 1.2.2 W/W emulsion formation in the gelatin/maltodextrin system (Esquena, 2016).

The segregative phase separation is mainly involved in the current study with a simplified model chosen to be analysed. We take the solution where there is no electrostatic interactions existing between components, which are incompatible electrically neutral polymers and solvent molecules.

A great deal work has attempted to predict the segregative phase separation. The Flory-Huggins interactions parameter is considered as a vital persuasive factor to discuss the system. The Flory-Huggins interactions parameter can numerically describe the strength of short ranged interactions between components in the polymer solution system to assist the theoretical estimation of predominance between attractive and repulsive force by comparing the polymer1-polymer2 parameter and solvent-polymer1, solvent-polymer2 parameters. When repulsive force is stronger than attractive force, two kinds of polymers tend to move to different phases resulting in the phase separation. Unfortunately, the limitation of this theory is that the larger ranged, such as

electrostatic intermolecular interactions are ignored so that discrepancy may occur between practical situation and theoretical predictions.

The work reported by Dickinson indicated that the conventional methods to stabilise O/W or W/O emulsions are not suitable for W/W emulsions. They are distinguished by interfacial tension, the bending rigidity and the interfacial permeability (Sagis, 2008) (Scholten et al., 2006a). The interfacial tension is describing the free energy per unit area of expanding the area of the interface between two adjacent separated phases. Compared to O/W emulsions, W/W emulsions possess far lower interfacial tension and stronger bending rigidity. And it has been measured that interfacial tension for water/gelatin/dextran and water/gelatin/gum arabic is only 10^{-3} mNm^{-1}, compared to 30 mNm^{-1} of O/W emulsions (Ding et al., 2002) (Scholten et al., 2006a). The very low interfacial tension tends to enlarge the spatial extent of the interface and finally might even exceed the size of conventional surfactant molecules. Due to the simultaneous presence of small solvent molecules and large polymer molecules on the water-water interface, not only the dispersed solvent molecules but also the dissolved large polymers are able to permeate through the interface gradually. Consequently, the above characteristics lead to the considerable broadening of the water-water interface order of magnitude thicker than traditional surfactant molecules. Unlike O/W systems, the surfactant molecules don't have sufficient length to probe both two adjacent phases to detect the presence of a true interfacial region. Hence, discovering new effective stabilising agents for W/W emulsion has attracted attention of lots of scientists. It is found reasonable to synthesise a kind of substance containing covalent bonds, with sufficient size having region attractable to polymers in both two phases (Dickinson et al., 2018). However, this technique remains difficult to realize in practice. There’s also another way involving creating an electrostatic macromolecular complex which has the analogical conformation with polymer A, and affinity to polymer B (Tromp et al., 2016). Yet, the most interesting and convenient method discovered recently is the addition of particles, in a manner similar with Pickering emulsions.

1.3 Bijel characters

Bijel is the abbreviation of Bicontinuous Interfacially Jammed Emulsion Gels. It refers to two phase systems containing bicontinuous biopolymer solution phases. And the bicontinuous conformation can be stabilised by the attractive force between sufficiently gelled material on the surface induced by the capillary attractions at the interface between these two phases. Biocontinuous emulsion can be obtained when the volume ratio of the two phases is close to 50:50, according to Figure 1.2.2. Bijel is closely related to the solution system studied in this work, and it seems to be related to W/W emulsion. However, they are actually different since W/W emulsions are not bicontinuous in the same way as bijels.

Phase separation occurs in bijel system as well due to high incompatibility of biopolymer components. Biopolymers commonly used to form the system are proteins and polysaccharides, most of which possess quite high molecular weight (M_w) and may be charged to influence the stability of the solution system. Proteins always have terminals with positive or negative charges and possible globular highly folded structures that can interact with other polymers, while the polysaccharides consist of longer chains, though they may helically fold as well. Polysaccharides can possess various charges depending on charge carrying groups, like carboxylate groups and sugar amine moieties, depending on pH conditions. The thermodynamic equilibrium can be affected by entropic and enthalpic fluctuations caused by these characteristics when proteins and polysaccharide, or two polysaccharide species, are mixed in the solution. Entropy can be affected when these macromolecules with distinct shapes mix together, and enthalpy can be impacted due to the interaction with charged groups of these different polymer species.

As mentioned above, there are two-phase separation types commonly existing in the polymer solution, referred to segregative phase separation and associative phase separation. Broadly speaking, associative phase separation typically does not arise in bijel system. Instead, segregative phase separation is always one that is required in the formation of bijels.

1.4 Particles performance and principles of using them for arresting polymer solutions (e.g. bijels)

Since conventional emulsifying agents are not able to increase the stability of the W/W emulsions and bijel, scientists have been searching for alternative approaches to achieve the task. The function of small particles on their ability for stabilising W/W emulsions has been proved in considerable detail and is attributed to the formation of the Pickering type emulsions and so-called Mickering emulsions. The difference is only about the material of from which the particles are formed. Pickering emulsions are formed by stabilisation by hard, non-deformable solid particles, whereas Mickering emulsions relate to soft, deformable microgel particles (Zembyla et al., 2018) (Stratford et al., 2005). The presence of particles of various materials at water-water interfaces, in mixed phase-separated polymer solutions offers the possibility of stabilisation. Firoozmand, Murray and Dickinson discovered that particles adsorbed at the interface do inhibit phase separation and provide valid evidence for feasibility of forming Pickering type W/W emulsions (Firoozmand et al., 2009). Prior to this, often the stabilisation of the system was only achieved by building stable networks of every polymer in the bulk phases and the formation of stabilising interactions between them.

Regarding how to stabilise the bijel system, the most direct way would be to synthesise a kind of substance composed of one of the biopolymer components in the solution connected to the other biopolymer in order to sit at the interface between the two phases. However, this procedure needs a complicated process to produce, test and improve. Fortunately, it has been known that small colloidal particles can also adsorb onto the material at the interface, promoting the blocking of the interface in order to increase the stability. The adsorption energy ΔE of a particle of radius R, attached to the interface between the two phases is given as (Levine et al., 1989)

$$\Delta E = \pi R^2 \gamma (1 - |\cos(\theta)|^2) \qquad (1.4.1)$$

In the above equation γ is the interfacial energy between the two separated phases while θ is the contact angle between spherical particle and two phases as Figure 1.4.1.

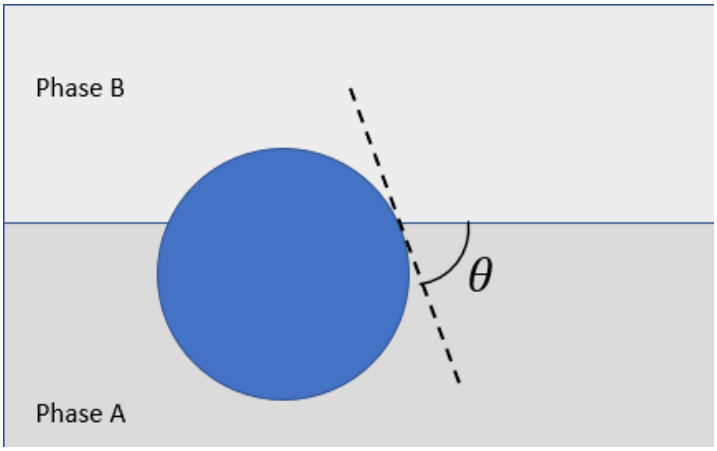

Figure 1.4.1 Particles at interface penetrating two phases and the contact angle θ is marked out.

Note that the essential condition for validity of this equation is that the particle is already attached to the interface. According to the above equation, it is evident that the size of the particles is a vital factor to influence detachment energy. The larger the particle is, the tighter the particles are bond to the interface between the two phases. On the other hand, contact angle θ is also closely related to the difficulty of removing the adsorbed particles and it depends on the difference in the interfacial tension of the surface of the particle (s) with the two liquid phases (γ_{sA} and γ_{sB}). It can be described by Young's equation (Makkonen, 2016):

$$cos\theta = \frac{\gamma_{sA} - \gamma_{sB}}{\gamma_{AB}} \qquad (1.4.2)$$

According to the equation (1.4.1) and (1.4.2), the detachment energy would be maximum when the contact angle is $90°$, i.e. when γ_{AB} is rather large compared to $(\gamma_{sA}-\gamma_{sB})$. The value of interfacial tension between two phases γ_{AB} has been measured ranging from 100 to 1 μNm^{-1} or even lower in many experimental studies involving phase separated polymer solutions (Scholten et al., 2006a). Therefore, it is of same importance to achieve $(\gamma_{sA}-\gamma_{sB})< \gamma_{AB}$, which ensure that the free energy change due to attachment is maximum. The following (Figure 1.4.2) indicates the relationship between θ and $\Delta E/k_BT$ when γ is set as 1 μNm^{-1}, k_B is the Boltzmann constant and T is the temperature in degrees Kelvin. The results are calculated according to equation (1.4.1).

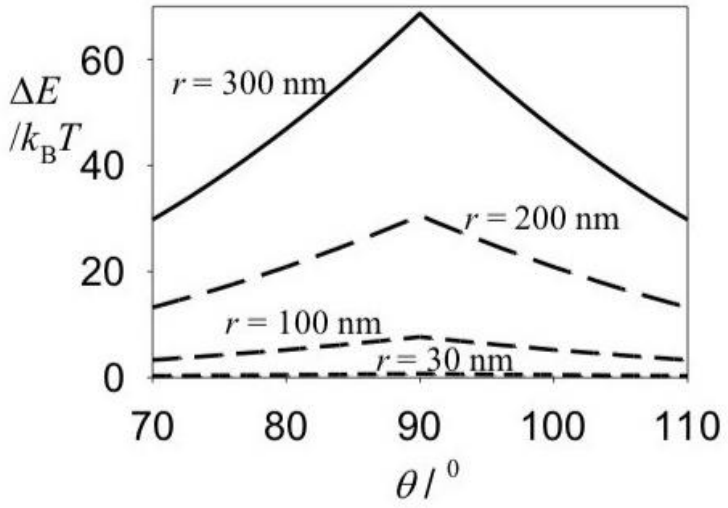

Figure 1.4.2 Changes in detachment energy of a particle from the interface as a function of the contact angle (Figure taken by Professor Brent Murray).

It is remarkable that the minimum Boltzmann weighting factor for immobilising adsorbed particle $\Delta E/k_BT$ is 2×10^3e, even for the smallest particles r ~ 30 nm. According to the Figure 1.4.2, when the interfacial tension is 1 μNm^{-1}, particles with radius of 100 nm and contact angle θ set to $90°$ need to obtain an energy above $7k_BT$ to detach itself from the interface. That is to say, most of the particles are regarded as being adsorbed on the interface more or less irreversibly, since they possess larger size and the interfacial tension is not likely to be much smaller than 1 μNm^{-1}. In addition, the contact angle θ when $90°$ provides the maximum value of the adsorption energy. Unless the system

is subjected to high shear forces or any other intensive treatments, the particles covering the interface would be stable enough not to be displaced from the surface. This contributes greatly to the stability of the structure of the bijel emulsion systems. Nevertheless, amongst these vital parameters, controlling contact angle is not so easy. In practical, contact angle is also not as trivial to measure and speculate since particles are always not present alone. Instead, groups of aggregated particles are usually found clustered together at the interface. Another complication is the affinity between particles and polymer molecules, which could strongly influence the contact angle θ. Proteins are prone to adsorption into the surface of the particles, hence leading to the tendency for particles to move into the phase enriched with protein, and it results in the change of θ and complete wetting of the particle by protein rich solution. A similar situation can also occur due to the charge of biopolymers which may interact with charged particles.

Dickinson reviewed several related studies in the literature and concluded that particle adsorption is substantially driven by thermodynamic principles and origins. When the system attempts to minimise its free energy by reducing the area of the energetically unfavourable liquid interface between the two incompatible phases. The mechanism of the instability of bijel is similar to the one for W/W emulsions or in Pickering-stabilized oil-water emulsions. The difference is that the particles-coated droplets tend to aggregate together in W/W emulsion. To impede the coalescence of the droplets and obtain the long-lasting stabilisation, the formation of a coherent thick layers at the interface by a surface active material is of significant importance (Dickinson et al., 2018).

Nowadays there exist a considerable choice of materials from which the stabilising particle agents can be constructed from. Microgel is popular in relevant experimental works. For example, polymer microgel particles were chosen to be added into solutions of poly(ethylene oxide) + dextran by Nguyen (Scholten et al., 2006a). Murray and Phisarnchananan introduced whey protein microgels into a solution of starch + locust bean gum, and found that this improved the particles stabilising function (Murray et al., 2014). Other

types of biopolymer conjugate particles, emulsion droplets, polymer lattices, inorganic particles and nanocrystals, bacterial cells have all been tried and recognised as useful materials for stabilisation of W/W emulsions, as well as bijel (Poortinga, 2008) (Balakrishnan et al., 2012) (Peddireddy et al., 2016).

1.5 Particles tendency for residing into one of the phases in polymer solution

An interesting phenomenon has been reported in several pieces of researches, where it is found that the particles tend to accumulate into one of the phases, but not the other, irrespective of how they are introduced into the system. Moreover, this continues to be the case even when both groups of polymers show no specific affinity towards the added particles. The experiments performed by Firoozmand, Murray and Dickinson indicates that when adding a certain kind of colloidal particles (amphoteric polystyrene latex) into the blend of gelatin and oxidised starch, a kind of thermodynamic driving force, referred to osmotic repulsion emerges between the particles and hydrophilic starch polymer molecules (Firoozmand et al., 2009). It is suggested that this makes the particles, at finite concentrations, preferentially aggregate at the liquid-liquid interface and the gelatin-rich region heated at 40 °. It was speculated by the authors that the property of viscoelasticity is the vital factor leading to the phenomenon. A work reported by another group to stabilize the W/W emulsion containing dextran and poly(ethylene oxide) by nanorods indicates that added particles strongly prefer to the dextran phase (Peddireddy et al., 2016). More experimental studies reported analogous situation irrespective of how particles are introduced into the solution. These researchers concluded that this phenomenon is relevant to the thermodynamic equilibrium state of the particles in the emulsion, rather than kinetic considerations. There is no doubt that added particles would prefer to be in the phase enriched with one of two types polymers if a certain kind of favourable interactions exist between the particles and only one of the polymer

species. Nevertheless, in most of these experiments various measures are taken to ensure that no specific interactions between the particles and the polymer solution exist in the system. Despite this, in many relevant reported works, the tendency for accumulation favouring one phase does not seem to disappear (Moschakis et al., 2006). The theoretical explanation to understand the phenomenon is what the study in this project will focus on.

1.6 Flory-Huggins theory

Flory-Huggins theory is the most well-known mathematical model for describing the change in the free energy of polymer solution system when different polymer species are mixed. It provides a quantitatively accurate interpretation of a broad range of experimental results. The theory has been applied in many pieces of research works, like the starch water mixture (Van der Sman et al., 2011). The Flory-Huggins theory is adopted as the vital part of mathematical tools in this project to speculate the mechanism of the phenomenon, in order to first calculate the compositions of the two coexisting phases.

The Gibbs free energy is related directly to the entropy and the enthalpy of mixing as following:

$$\Delta G_{mix} = \Delta H_{mix} - T\Delta S_{mix} \qquad (1.6.1)$$

$\Delta G_{mix}$is the Gibbs free energy, ΔH_{mix} is the enthalpy, and ΔS_{mix} is the entropy of the thermodynamic system. The entropy of the mixture implies the increase of the uncertainty about the locations of the molecules when they are interspersed. In other words, entropy is regarded as a quantitative measure of disorder and the degree of randomness. The larger the entropy, the higher the disorder. As for the enthalpy, this is the sum of the internal energy and product of its pressure and volume in a thermodynamic system. Flory and Huggins gave the explicit formula for ΔH_{mix} and $T\Delta S_{mix}$ (Flory, 1953), leading to

$$\Delta G_{mix} = RT[n_1 In\phi_1 + n_2 In\phi_2 + \phi_1\phi_2\chi_{12}] \qquad (1.6.2)$$

In this formula, n_1 is the number of moles and ϕ_1 is the volume fraction of solvent, n_2 and ϕ_2 is the number of moles and volume fraction of polymer. Only the solvent and one type of polymer molecule is considered here, as the simplest model to explain the basic principal of the Flory-Huggins theory. Later of course we consider cases involving multiple polymer species. In equation (1.6.2), R is the gas constant, and T represents the absolute temperature. The quite important interaction parameter χ was introduced by Flory and Huggins to describe the degree of incompatibility of dispersing polymers and solvent molecules in their lattice model of polymer solutions. This parameter provides a numerical description of mutual miscibility between every pair of various type of component molecules and accounts for the short ranged interaction between different species (i.e. monomers that make up the polymer chains, both amongst themselves and with solvent molecules). In a well-dispersed solution, χ between polymer molecules and solvent molecules ought to be small to satisfy the condition for polymer molecules to expand and dissolve in the solvent. Such solvent is a good solvent for the polymer. In contrast, when χ reaches a certain value, which depends on the varieties of polymers, the repulsive force between polymer and solvent molecules becomes large enough to avoid contact with each other leading to the immiscible situation. The threshold value separation the two types of solvents is c = ½. At this value of c the solvent is referred to as a q-solvent. The configuration of polymer chains takes on what is known as ideal chains (rather than swollen chains) at this c value. In this case we are said to have a poor solvent. The interaction parameter is often considered as consisting of two parts

$$\chi = \chi_H + \chi_S \qquad (1.6.3)$$

Literally, they refer to the enthalpic part and entropic part, respectively. The entropic part can be derived from the random dispersion of monomers (i.e. a system of free monomer solution that have not formed a polymer chain). The interaction parameter mainly depends on the temperature and degree of polymerization, the concentration of polymer solution.

$$\chi(T) = A + \frac{B}{T} \qquad (1.6.4)$$

Combined with the equation (1.6.3), the term involving “A” matches the enthalpic part and the one with “B” corresponds to the entropic part. According to the equation (1.6.4), the parameter is a linear function of the inverse ambient temperature. Cases where $\chi = 0$, independent of temperature are known as “athermal solvent”. To conclude, in the environment with a given ambient temperature, fixed concentration and total composition of polymers, the interaction parameter between two polymers is not prone to change. More details of the Flory-Huggins theory will be discussed in the model and methodology part in a later chapter.

1.7 Self Consistent Field (SCF) calculations

Self Consistent Field calculations, often implemented on a lattice model, is utilized here to simulate the distribution profile of different components in a polymer solution when the system is in thermodynamic equilibrium. Components in polymer solution are basically polymer molecules, having high molecular weights, some small mobile ions and solvent molecules. Though in the purpose of this study we consider non-charged polymer species and therefore also no ions in the solution.

The SCF calculation was originally implemented by Dolan when investigating polymer distribution and interaction between two plain surfaces on to which polymer chains are adsorbed by one end, only (Dolan et al., 1975). The model was constructed to describe the space between two plain surfaces in the origin implementation of SCF. It has been improved further by Scheutjens to allow more complex situation involving a larger variety of polymer structures (Scheutjens et al., 1979). With this more recent version it is also possible to evaluate the number of tails, loops and trains. They derived the partition function of segments of polymers and their distribution behaviour to assist

investigating the emulsifying and stabilising capacity (Scheutjens et al., 1979) (Scheutjens et al., 1980). The developed model system acts as an analysing tool for the extended range of polymer types, such as homopolymers in a binary solution (Bohmer et al., 1990) and polyelectrolyte between two parallel surfaces (Pryamitsyn et al., 1996). For instance, Dickinson utilised SCF models to calculate and analyse the differences between conformational properties of adsorbed β-casein protein layers at oil/water and air/water interfaces (Dickinson, et al., 1993). The practicability of the SCF calculation in predicting the behaviour of polymers at interfaces has been proved in a variety of theoretical studies (Leermakers et al., 1996) (Ettelaie et al., 2014b) and the development of SCF calculation is still on going to include even more complex situations.

In the present study, to obtain theoretically the distribution profile of varying species in the polymer solution, SCF calculation is applied to simulate the interface of a solid in contact with bulk liquid consisting of each of the two phase-separated solutions. We obtain the density profile variation of each component in the solution as a function of distance away from the interface. Furthermore the free energy can be inferred. Thus, the numerical conclusion leads to results that support and allow an understanding of phenomenon of fractionation of particles in polymer solution.

1.8 Konjac gum and *κ*-carrageenan

Konjac gum and κ-carrageenan are two kinds of hydrocolloids chosen to manifest the phenomenon that introduced particles favour one phase in polymer solution. Fluorescent latex is adopted as the added particles in the experimental part of the present work. As hydrocolloids, Konjac gum and κ-carrageenan are natural long-chain polymers with high molecular weight. They play a vital role in improving food quality in food-related industries and chemical engineering by thickening and imparting viscosity (Glicksman, 2019).

Konjac gum, which comprises 60-70% konjac glucomannan, can build up strong elastic gels to increase the viscosity of blended systems (Al-Ghazzewi et al., 2007). Furthermore, it is able to assist improving the texture of the product. Konjac gum can be utilized as ingredients of traditional Chinese medicine in China as well due to its health benefits (Yaseen et al., 2005). The molecules of Konjac gum is formed by connecting mannose and glucose units in a ratio of 1.6:1. And these units are combined with $\beta\,(1,4)$ linkages as shown in Figure 1.8.2 (Takigami, 2009).

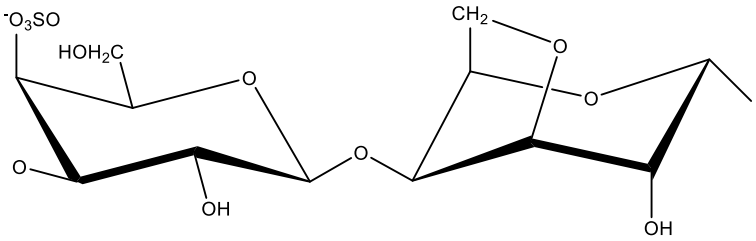

Figure 1.8.1 Chemical structure of the repeating unit of κ-carrageenan (Morris et al., 1980).

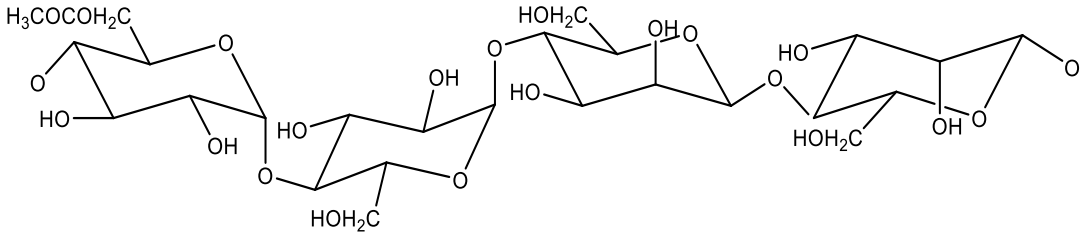

Figure 1.8.2 Chemical structure of the repeating unit of konjac gum (Takigami, 2009).

Carrageenan is generally extracted from marine red algae and it is a family of linear sulphated polysaccharides. Advantage is taken of its properties in controlling moisture and stability of the food products due to its function at behaviour to promote gel formation. The family members are distinguished by degree of sulfation, and κ-carrageenan is a linear polysaccharide formed of repeating combined units of 3-linked-β-D-galactose-4-sulfate and 4-linked-3.6 anhydro--α-D-galactose as displayed in Figure 1.8.1 (Morris et al., 1980).

Special conformational transition from coil to helix construction appears with helix aggregation contributing to its gelation property (Daniel-da-Silva et al., 2011).

Konjac gum and κ-carrageenan can be mixed together to enhance the function of thickening and gelation (Majzoobi et al., 2017) has tested the addition of these two hydrocolloids in meat substitutes and found significantly improved overall quality of meat-free sausages. They are beneficial for increasing the hardness, reducing frying loss, improving water-holding capability and lightness of each food products.

The present work utilizes the phase separation phenomenon as if occurs in a solution containing the above two polysaccharides to examine the tendency for introduced particles to accumulate in one phase but not the other. This system is chosen as there is no specific significant interactions between the particle surface and these two polysaccharides to enthalpically influence the preference of particles for one phase or the other phase.

Chapter 2
Methodology

The present study applies the numerical technique, based on Self Consistent Field (SCF) calculations, to a variety of two phases systems to determine the interfacial properties of these systems. The numerical computer program assists to obtain information on phase behaviour of polymer mixed solutions of the simplified model and to calculate interfacial energies of solid substrates in contact with each of the two co-existing phases. The data from the output files generated by the program is further analysed in Microsoft Excel software, version 2010. In absence of an interface, spatial distribution of polymers is homogenous within each phase. Presence of a hard surface, into which polymers cannot penetrate, alter this uniform distribution. In this chapter, the calculation principle and the details of our simplified model is specifically discussed, accompanied by the material and methods for experimental part of the work.

2.1 The process of calculation

To achieve the confirmation of the model, what should be done first is to figure out the process of the simple model as Figure 2.1 in order to make changes more clearly. The overall process of calculation can be divided into two parts. The first part is to determine the phase separation and its composition, and the second part is calculating the interfacial tension in the solution system when particles are introduced in it and predict their tendency.

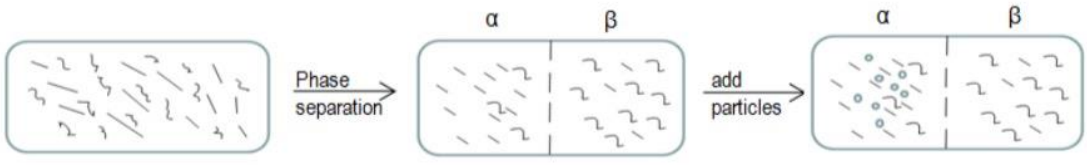

Figure 2.1 The process of imitation model

2.2 Application of Flory-Huggins theory in the current

Here we exhibit the calculation principle for obtaining the concentration of each polymer in each of the two co-existing phases. This needs to be done before we can apply SCF calculation to each phase. According to the Flory-Huggins theory (Flory, 1953), the free energy of a mixed polymer solution system in the case considered here can be expressed as

$$\frac{F}{k_b T} = \frac{\phi_S}{1}\ln\phi_S + \frac{\phi_1}{N_1}\ln\phi_1 + \frac{\phi_2}{N_2}\ln\phi_2 + \chi_{12}\phi_1\phi_2 \qquad (2.2.1)$$

In this equation, ϕ_S, ϕ_1, ϕ_2 represent the volume fractions of solvent and polymers 1 and 2, respectively. The symbols N_1 and N_2 represent the degree of polymerizations, expressed as the size of polymers (or the number of repeat monomers units). T is the temperature and k_b the Boltzmann constant. The interaction parameter χ describes the incompatibility of two polymers. According to the same model as that to be used for the SCF calculation, the solution is considered as divided into cubic lattices points each with a size of a_0, making the free energy F in equation (2.2.1) as that per a volume of size ${a_0}^3$, in bulk solution. The above formula is produced in the following way. At first, from the definition of Gibbs free energy, its value for the mixture is related to enthalpy and entropy of the system:

$$\Delta G_{mix} = \Delta H_{mix} - T\Delta S_{mix} \qquad (2.2.2)$$

The entropy of the polymer solution can be expressed as the following, when this represents entropy of mixing of all three components together:

$$\Delta S_{mix} = -k_b\left(\frac{\phi_1}{N_1}\ln\phi_1 + \frac{\phi_2}{N_2}\ln\phi_2 + \phi_S\ln\phi_S\right) \qquad (2.2.3)$$

While the enthalpy of the mixing is obtained as following

$$\Delta H_{mix} = k_b T(\chi_{1S}\phi_1\phi_S + \chi_{2S}\phi_2\phi_S + \chi_{12}\phi_1\phi_2) \qquad (2.2.4)$$

Thus, combining the above three equations one finally arrives at the free energy of the solution system, which turns out to be

$$\frac{F}{k_b T} = \frac{\phi_S}{1}\ln\phi_S + \frac{\phi_1}{N_1}\ln\phi_1 + \frac{\phi_2}{N_2}\ln\phi_2 + \chi_{1S}\phi_1\phi_S + \chi_{2S}\phi_2\phi_S + \chi_{12}\phi_1\phi_2 \quad (2.2.5)$$

where of course $\phi_S = 1 - \phi_1 - \phi_2$. However, as mentioned before, we take the solvent to be a good solvent for both sets of polymers in the solution, implying a low or even negative values of χ_{1S} and χ_{2S}. For simplicity we take the solvent to be an athermal one, i.e interaction parameter $\chi_{1S} = \chi_{2S} = 0$ here. In the end, with this assumption, the free energy equation simplifies and becomes just the one shown in equation (2.2.1).

2.3 Phase separation determination

Phase separation is the first part in the process of overall calculation. In this model, there is a solution system including two species of polymers labelled here as 1 and 2 with initial overall volume fractions of ϕ_1^{ini} and ϕ_2^{ini}, set in advance. There is no charged electrically relevant interactions considered to exist in the solution, with polymers being made of neutral monomers. Only some relatively weak and necessary interactions characterized by Flory-Huggins parameter χ between the two types of polymers are included. Being placed for a sufficient long time at room temperature, this system can in principle phase separates into two distinct phases when its composition corresponds to the situation above the binodal curve in the phase diagram, denoted as phase α and β. Two polymers separate spontaneously and go to different phases if the χ_{12} is sufficiently unfavourable (i.e. positive). Polymer 1 primarily goes to the phase α, in contrast, polymer 2 mainly goes to the phase β. Nevertheless, a small amount of each kind of polymer may also be found

in the opposite phase as well, particularly where χ_{12} is just sufficiently large enough to cause incompatibility.

As the total amount of two sets of polymers are fixed in the overall system and are not going to increase or reduce during phase separation, the initial volume fraction of each polymers equals to the total fraction volumes in two phases following the phase separation, after taking the volume fraction of each phase into account. This consideration for each polymer gives two further equations:

$$\phi_1^{ini} = \upsilon\phi_1^{\alpha} + (1-\upsilon)\phi_1^{\beta}, \quad \phi_2^{ini} = \upsilon\phi_2^{\alpha} + (1-\upsilon)\phi_2^{\beta} \qquad (2.3.1)$$

In the above equations, ϕ_1^{ini} and ϕ_2^{ini} indicate the initial overall volume fraction of polymer 1 and polymer 2, respectively. Similarly, ϕ_1^{α} and ϕ_2^{α} represent the volume fractions of polymer 1 and polymer 2 in phase α, ϕ_1^{β} and ϕ_2^{β} denote the volume fractions of the two polymers in phase β. υ is the volume fraction of phase α, which leads to the volume fraction of phase β as (1- υ).

To make further progress we first need to provide an explanation of the term chemical potential. It describes the free energy change of the thermodynamic system due to a change of the molar amount in it. Thus, at equilibrium, the chemical potential of the same species of polymers will not change and has to be the same in both opposing phases. At equilibrium the chemical potential of all three components, polymer 1, polymer 2 and solvent has to necessarily be the same in both phases. Therefore, here we can get three equations to describe the equality of these chemical potentials.

$$\mu_{\alpha}^{1} = \mu_{\beta}^{1}, \qquad \mu_{\alpha}^{2} = \mu_{\beta}^{2}, \qquad \mu_{\alpha}^{S} = \mu_{\beta}^{S} \qquad (2.3.2)$$

Meanwhile, the calculation method for chemical potentials of two categories of polymers is shown as the following equations.

$$\mu_1 = f(\phi_1, \phi_2) - \phi_2 \frac{\partial f}{\partial \phi_2} + (1-\phi_1)\frac{\partial f}{\partial \phi_1}$$

$$\mu_2 = f(\phi_1, \phi_2) - \phi_1 \frac{\partial f}{\partial \phi_1} + (1 - \phi_2) \frac{\partial f}{\partial \phi_2} \qquad (2.3.3)$$

Similarly, the chemical potential of solvent can be shown to be (Ettelaie et al., 2019)

$$\mu_0 = f(\phi_1, \phi_2) - \phi_1 \frac{\partial f}{\partial \phi_1} + \phi_2 \frac{\partial f}{\partial \phi_2} \qquad (2.3.4)$$

In the above equations, f represents the function of the free energy of solution per unit volume relating to the proportion of two polymers in solution. It can possess complicated descriptions depending on the particular situation and many forms for f has been suggested. However, in this simplified model f is expressed as

$$f = \frac{\phi_1}{N_1} \ln \phi_1 + \frac{\phi_2}{N_2} \ln \phi_2 - (1 - \phi_1 - \phi_2) \ln(1 - \phi_1 - \phi_2) + \chi_{12} \phi_1 \phi_2 \quad (2.3.5)$$

where N_1 and N_2 indicate the degrees of polymerization, which describes the size of polymer chain of polymer 1 and polymer 2. The form of f chosen is from the Flory-Huggins theory we discussed in equation (2.2.1). Now we have got five unknown variables $\phi_1^\alpha, \phi_2^\alpha, \phi_1^\beta, \phi_2^\beta$ and υ appearing in the above set of equations (2.3.1) and (2.3.2). The target is to figure out the final distribution situation of the solution system, such as it separates into two phases or whether the system remains a single phase. Thanks to the existence of equation (2.3.1), variables $\phi_1^\beta, \phi_2^\beta$ can be expressed as $\phi_1^\beta = \frac{\phi_1^{ini} - \upsilon \phi_1^\alpha}{1 - \upsilon}$ and $\phi_2^\beta = \frac{\phi_2^{ini} - \upsilon \phi_2^\alpha}{1 - \upsilon}$. Thus, there are only three variables $\phi_1^\alpha, \phi_2^\alpha, \upsilon$ left to be determined, since ϕ_1^{ini} and ϕ_2^{ini} are initial volume fractions of two polymers and are known in advance. These equations can be solved numerically by the application of multidimensional Newton-Raphson method or the conjugate gradient method, such as the one in MINPACK library, which focus on issues of simultaneous nonlinear equations (Ziegel, 1987). Therefore, we are able to solve and calculate volume fractions of each kind of polymer in each of the two co-existing phases, as well as the proportions of each phase, υ and $1 - \upsilon$.

2.4 SCF Calculations

The Self Consistent Field (SCF) numerical calculations allow for the variation in the volume fraction of each polymer present in a phase, to be monitored as a function of distance away from a solid interface. It can equally be applied to the gap between two solid particles very close to each other, such that their adjacent surfaces at the point of close approach may be regarded as two parallel plain walls as Figure 2.4.1.

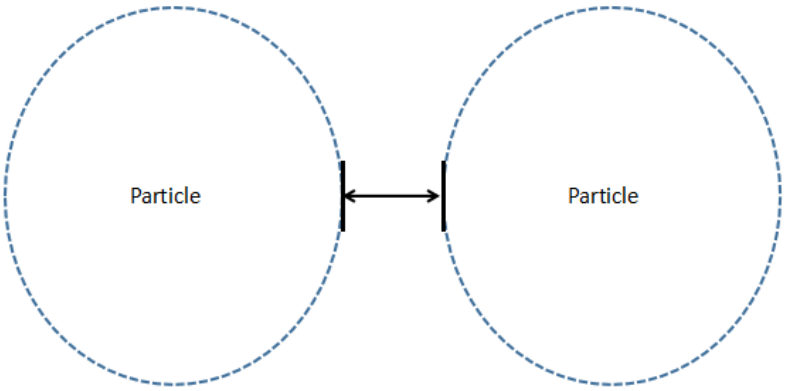

Figure 2.4.1 Two approaching particles and the adjacent surface can be regarded as two plain walls.

The gap region between these two surfaces is evenly divided into a large number of grid points on a cubic lattice, which each lattice point occupied either by a monomer, belonging to a chain of polymer, or a solvent molecule as is shown in Figure 2.4.2. To calculate the distribution of polymers segments in a phase, numerical parameters of distance and layers between two adjacent walls are set. In this study, the bulk of solution next to the solid particle surface is considered as a large number of particle layers, placed increasing away from the surface. Meanwhile, lattice spacing as well as thickness of layers a_0 is taken to be 0.3 nm, the size of a carbon-carbon bond

by Scheutjens and Fleer (Scheutjens and Fleer, 1979) or indeed particle bond in proteins. We consider 180 layers (z=180) corresponding to 54 nm as the largest distance away from the surface.

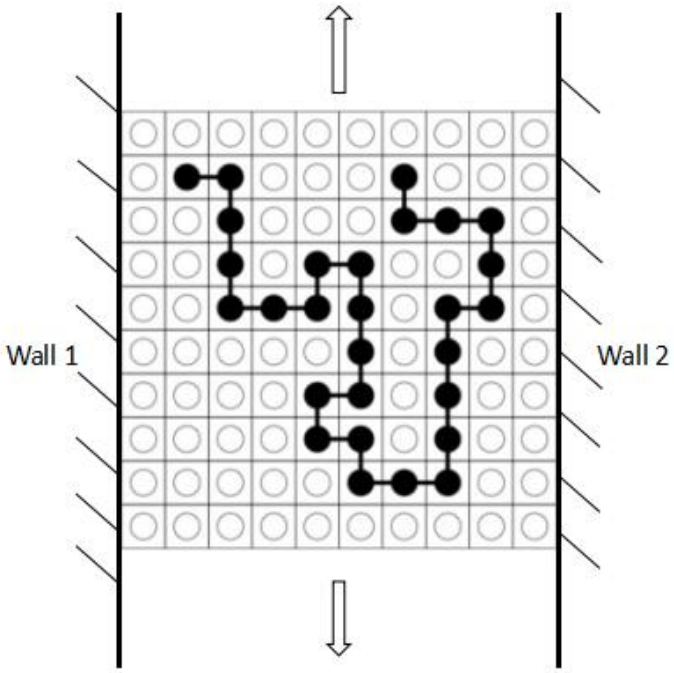

Figure 2.4.2 Illustration of a part of the lattice model used for SCF calculations. The white circles represent solvent molecules and the black circles linked represent the polymer monomers.

This distance is in past limited by the computer memory limits and the time it takes for programs to converge. At the distance of 54 nm from the solid surface, any disturbance from the surface should have died out. Thus, the space next to the surface of solid particles is approximately recognized as a 180 x 180 square area, with each lattice of 0.3 nm x 0.3 nm. In practical, polymer molecules dispersing in solution are unequally located in these cubic lattices. The major focus of the SCF calculations is to determine the density profile distribution of polymers, for which the free energy of the system is at a minimum.

As well as determining the polymer density profile, the task of SCF is also to determine the change of free energy with the variation in the gap size between the two solid surfaces. Though in present study, we mainly focus on behaviour

of single surface (or two surfaces far apart). Nevertheless, the free energy does not always remain invariable and it fluctuates with concentrations of polymer molecules at any certain location in bulk solution. SCF calculations determine the most probable concentration profile which lead to minimum free energy for the system. Regarding as to how to obtain the minimum value of the free energy, SCF runs iteratively to test every point located next to the solid surface, which is set as cubic lattice in the model, in the bulk solution. During the iterations, the composition in divided layers are varied systematically and the corresponding free energy is decreased commensurately. The iterations do not stop until the minimum free energy has been found for the given desired gap size. Equation (2.2.1) can be generalized to situation involving a non-uniform variation of the polymer density profile. It provides the free energy for a uniform distribution of polymers and is mainly related to the volume fractions of each components in solution. As a matter of fact, there are a set of auxiliary fields $\psi_{\mathrm{i}}(r)$ (i=1, 2, and s), which also enter the equation for such generalized case. When the minimum point is reached, $\psi_{\mathrm{i}}(r)$ can be shown to take on the following value (Ettelaie et al., 2014a)

$$\psi_{\mathrm{i}}(r) = \psi_{\mathrm{h}}(r) + \sum_{j \neq i} \chi_{ij}\left(\phi_j(r) - \phi_j^{ini}\right) \qquad (2.4.1)$$

Where $\psi_{\mathrm{h}}(r)$ is termed as a Lagrange multiplier, describing the hardcore potential of polymer monomers and solvent molecules. It ensures the invariable total quantity of polymer + solvent at any layer r of bulk solution. In other words, it ensures the incompressibility of the solution and satisfies the relationship expressed as following (Ettelaie et al., 2014b):

$$\sum_i \phi_i(r) = \sum_i \phi_i^{ini} = 1 \qquad (2.4.2)$$

Then for the rest part of the right-hand side in equation (2.4.1), this represents the field that relates to concentration (volume fraction) configuration of surrounding components around any monomers. It is the combination of interactions occurring between any monomer species and its neighbouring

ones. Polymer chains tend to avoid the solid surface due to the entropy loss that they suffer when close to the surface. The same entropy consideration induces the polymers to stretch and extend away from the surface. This results in a depletion region next to the solid surface. At distances further from the solid surface, the volume fraction of polymers gradually goes up and becomes constant the bulk concentration when far away from the interface. The model utilized in the study is simplest exhibiting the phenomenon investigated here. The interactions between solvent and polymer monomers are ignored, leading to $\chi_{iS} = 0$. That is to say, the solvent is athermal one for both polymers. In contrast, χ_{12}, which describes the interaction between polymer 1 and polymer 2, plays a vital role as it needs to be sufficiently unfavourable to induce phase separation.

$\psi_{\mathrm{i}}(r)$ and $\phi_i(r)$ collaborate to assist SCF calculations find the point with minimum free energy in bulk solution next to the particle interface. At first, it was given a group of assumed value of $\psi_1(r)$. Then the corresponding $\phi_1(r)$ can be obtained in this condition by the segment density distribution functions derived from Scheutjens and Fleer (Scheutjens et al., 1979). The newly obtained $\phi_1(r)$ would now provide a new set of $\psi_2(r)$, by applying the equation (2.4.1). This process is repeated iteratively resulting in updates to $\psi_{\mathrm{i}}(r)'s$ and $\phi_i(r)'s$, and ends when the two sequential calculated values of $\psi_{\mathrm{i}}(r)'s$ or $\phi_i(r)'s$ are nearly equal to each other. In other words, it is said that 'self-consistent' has been achieved. It can be shown as well that free energy at this point reaches the minimum value, and it does not change with further iterations. Regarding to the method of calculation for free energy, and determination of $\phi_i(r)$ from $\psi_{\mathrm{i}}(r)$ at each step, we refer the reader to many excellent articles on this subject (Fleer et al., 1987) (Fleer et al., 1993).

2.5 Calculation for interfacial tension and particles tendency prediction

This is the second part of the overall calculation. In this stage, the phase separation has been determined and composition of solution system is known. Now if otherwise inert particles, with no specific interactions with either polymer 1 or 2, were to be introduced into the system, they interestingly are discovered experimentally to accumulate into one of the two phases as the Figure 2.1, but not the other. This step is to figure out the free energy per unit area change occurring in the solution system when particles are introduced in it.

This situation corresponds to the model built in SCF calculations, as discussed in 2.4, to determine the density profile of polymers next to the solid surface of the added particles, for which free energy is minimized. Meanwhile, the basic condition is that there is no specific interaction occurring between both two types of polymers and added particles such that the particles on the face value show no preference for any phase enriched with one kind of polymer or the other. The implementation of SCF calculation was introduced in 2.4. The iterations keep operating to find the point with minimum free energy in the solution. In the present work, the free energy per unit area of creating a solid interface in each of the two phases can be derived from this SCF computer-based calculations. Furthermore, once there are known, the relationship between free energy and the ratio of concentration of particles in the two phases is given according to Boltzmann distribution, i.e.

$$\frac{N_1}{N_2} = e^{\left\{\frac{-F(N_1)-F(N_2)}{kT}\right\}} \qquad (2.5)$$

This of course not only involves the interfacial energy (free energy per unit area a_0^2) of introducing a solid surface in each of the above two co-existing phases, but also the total surface area of the particle, when obtaining $F(N_1)$ and $F(N_2)$. The proportion of two polymers with different monomer number indicates whether the particles prefer to accumulate in the phase with larger polymers or the one with the shorter ones, if showing any tendency for fractionation at all.

Different situations with various variables like polymer size, interaction parameter χ and initial proportion of two polymers, as well as the construction of polymer chains would lead to more interesting consequences, which are going to be discussed in the next chapter.

2.6 Numerical calculation programs

There are a few input files involved in the running of the computer simulation programs. First stage of the calculations, as described in section 2.3, involves obtaining the composition in the phase separated system, establishing of such process occurs or not in the first place. This is done by solving equations (2.3.1) to (2.3.5). The corresponding input file demonstrates the degree of polymerization of each polymer. Meanwhile the initial volume fractions of polymers in the bulk solution should be specified also in the input file. The interaction parameters between two polymers need to be declared as well. Output file updates when program ends running, stating changes of volume fractions of both two polymers in each separated phase as well as the proportion of phases in solution system. Thus, the final distribution results are obtained.

Then we could move forward to next computer program which applies SCF calculations to determine the interfacial energy for every phase in phase-separated solutions, in contact with solid surface. Similarly, the input file indicates the total amounts of free linear polymers (ones that can exchange freely between the interface and the bulk solution), and the type and number of monomers in each polymer, followed by volume fractions of two polymers in phase α or β as determined from the previous stage of the calculations described above. The interaction parameters between monomers, monomers and solvent are demonstrated also included. After completion of the calculations, the output file updates to display changes of volume fractions of components in solution system and free energy in each case. Free energy calculation requires a knowledge of solvent and polymer depletion or

enhancement at the interfacial region, the internal interaction energy, and information on fields $\psi_i(r)$ discussed in section 2.4. Finally, these data will be used to obtain graphs to illustrate the relationship between polymer volume fraction and degrees of polymerization, free energy and interaction parameters, free energy and initial proportion of two polymers. Meanwhile the calculation, performed separately for each phase, can demonstrate whether differences in the free energy $F(N_1) - F(N_2)$, resulting from the depletion of polymers around particles, are responsible for particles partitioning tendency seen between the two phases, as seen by experimental researchers (De Gennes et al., 1979) (Mao et al., 1995).

2.7 Experimental aspects

In this part, we choose two kinds of incompatibles water-soluble polysaccharides konjac gum and kappa-carrageenan as the polymers to make up polymer solution. The fluorescent particle used in the experiment is COOH-PS microspheres labelled with Surface Green. The objective is to determine the concentration groups of two polysaccharide solutions that could induce phase separation phenomenon. And we can verify the accumulation tendency of introduced fluorescent particles in two separated phases.

Materials

Konjac Gum E425i (KG), product code 12190, was purchased from Ingredients (Hampshire, UK). Carrageenan E407 (K-C), product code E610933, was purchased from Special Ingredients (Chesterfield, UK). COOH-PS microspheres labelled with Surface Green, diameter 0.21 μm , was obtained from Bang Laboratories (Fishers, USA). All polysaccharide mixtures were prepared in the distilled water purified by treatment with a Milli-Qapparatus (Millipore, Bedford, UK).

Preparation of solutions and mixtures

Solutions of the konjac gum were prepared by dissolving the konjac gum powder in distilled water, then it is heat in water bath at 90℃ for about 1hr with constant manually stirring. Solutions of the κ-carrageenan were prepared by dissolving the κ-carrageenan powder in distilled water, then it is heat in water bath at 90℃ for about 1hr with constant manually stirring. The concentrations of these prepared two gums solution are ranging from 0.1wt% to 1.0 wt%, and all of them are placed in the cupboard at room temperature for 24hrs. Every concentration of one kind of gums solution is blended with another gum solution ranging from 0.1wt% to 1.0 wt% of the equal volume in the tubes, respectively, followed by heating in the water bath at 90℃ and automatic vibrating for 1hr. Afterwards, leave them in the room temperature for 24hrs and observe the phenomenon occurs next day.

Determination of phase separation and phase diagram

Phase separation can be observed and determined roughly first by eyes since two phases are apparently different, if so, light microscopy is applied to take images of two phases, respectively. Microscopy images for two solution before mixing were taken in advance. Thus, compare images before mixing and two phases after phase separation, every phase and polysaccharide can be matched. According to the phenomenon occurs next day in blends with various concentration groups, phase diagram for mixtures of konjac gum and κ-carrageenan can be drawn to find the region where phase separation takes place, and the corresponding concentration groups.

Introduction of fluorescent particles and confocal microscopy

Fluorescent labelled microspheres are added at a concentration of 0.2 vol.% into 5 ml κ-carrageenan solution with a certain concentration, and then add the same volume of konjac gum solution with a certain concentration. To eliminate the influence of sequence of two solutions, another sample with the same composition is prepared but add κ-carrageenan solution after the addition of particles in konjac gum. It should be noticed that the concentration groups chosen are those that have been proved to be phase-separated under

same condition. The mixtures are heated in water bath at 90℃ for 1hr as well to ensure the introduced particles are free and promoted to disperse randomly in solution. Afterwards, put the blends at room temperature for 24hrs and observe them the following day. Once the phase separation occurs, take a part of both the upper phase and the lower phase into laboratory-made well slides for confocal microscopy. A Zeiss LSM880 + Airyscan Upright Confocal Microscopy is operated in fluorescent mode with 10x EC Plan-Neofluor objective and 20x Plan-Apochromat objective. The images obtained would display the distribution situation of fluorescent particles in upper and lower phases, respectively. Compare images of these two phases in mixtures with different concentration groups, more conclusions can be derived to assist the theoretical inference.

Chapter 3
Result and discussion

In this chapter, the influence of various factors, such as degree of incompatibility, size of polymer, and the initial volume fraction of polymers in phase-separated solution system has been discussed. Furthermore, we explore the tendency of the added inert particles to partition predominantly into one phase or another. This is discussed theoretically numerical by calculations first and then the experimental facts which support the theoretical results for the preference of fluorescent particles for each of the two phases, enriched with two incompatible polysaccharides are considered.

Theoretical aspects

3.1 Depletion of one single kind of polymers around particles

To begin with, we are interested in depletion phenomenon of one single kind of polymer around solid particles, leading to the free energy differences which we believe are responsible for the preferential partition to one of the phases. To learn more about the principle and discuss the likely influencing factor, the polymer size has been changed to find the relationship between polymer distribution profile and the polymer size. The distribution profile can be described by polymer volume fraction changes as on moves away from the solid particle surface. Here, for the purpose of demonstration, it is set in the region between two solid surfaces to make the depletion effect more obvious. The computer simulation system applied with Flory-Huggins theory and SCF calculation can imitate the final stage of the distribution. In this initial simple example, it is assumed that only two components exist in solution, namely one kind of polymer and solvent molecules.

The calculated changes of volume fraction of a single kind of polymer on its own in the solution, within the gap between two approaching solid surfaces, is plotted as a function of distance away from the surface of one of the particles and is shown in figure 3.1.1. The unit of distance here are taken to be of 0.7nm,

which is numerical size of a single monomer a_0. As the graph shows, when the two particles are far apart, in the regions in the gap far from the surfaces, polymer volume fraction is identical to its bulk value. However, the closer one gets to either of the two surfaces, the smaller the polymer concentration becomes. As a result, there is clearly a depletion region around particles with a greatly reduced amount of polymer. Polymers close to an impenetrate surface lose substantial degrees of freedom since the number of configurations they can take is much more restricted compared to that they can adopt in bulk solution. In addition. There is no specific affinity between polymer and solid surface to compensate for the loss of entropy. This decreases in configurational entropy is the reason why polymers avoid the regions close to surface. Four lengths of polymer chains are chosen, the monomer numbers of them are 100, 200, 300, 500 and 700. There is no specific interaction between polymer and solvent, so interaction parameter is zero. The depletion area occurs in the distance range of around $10a_0$ similarly for all the polymers. As the number of monomers in polymers increases, the depletion area gradually increases. It seems that larger polymers have the stronger tendency to avoid the solid surface.

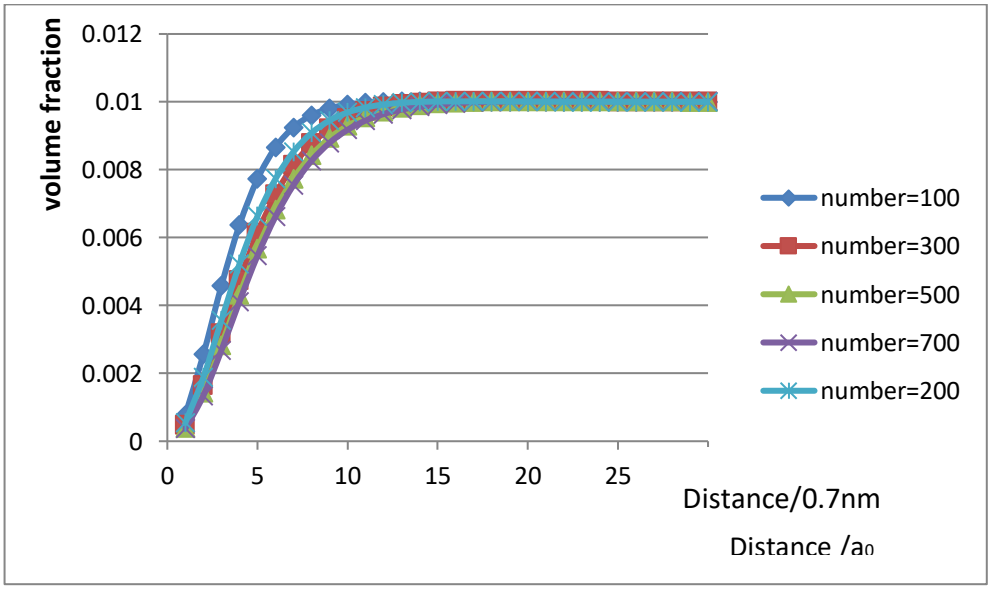

Figure 3.1.1 Volume fraction changes with increasing distance for polymers of different sizes.

Then the interfacial energy of particles was calculated and analysed. The interfacial energy is defined as the free energy needed for breaking the attractive force bonds between molecules to create a new surface. In this study, it is the free energy change of introducing a solid surface into the solution per unit area of created interface.

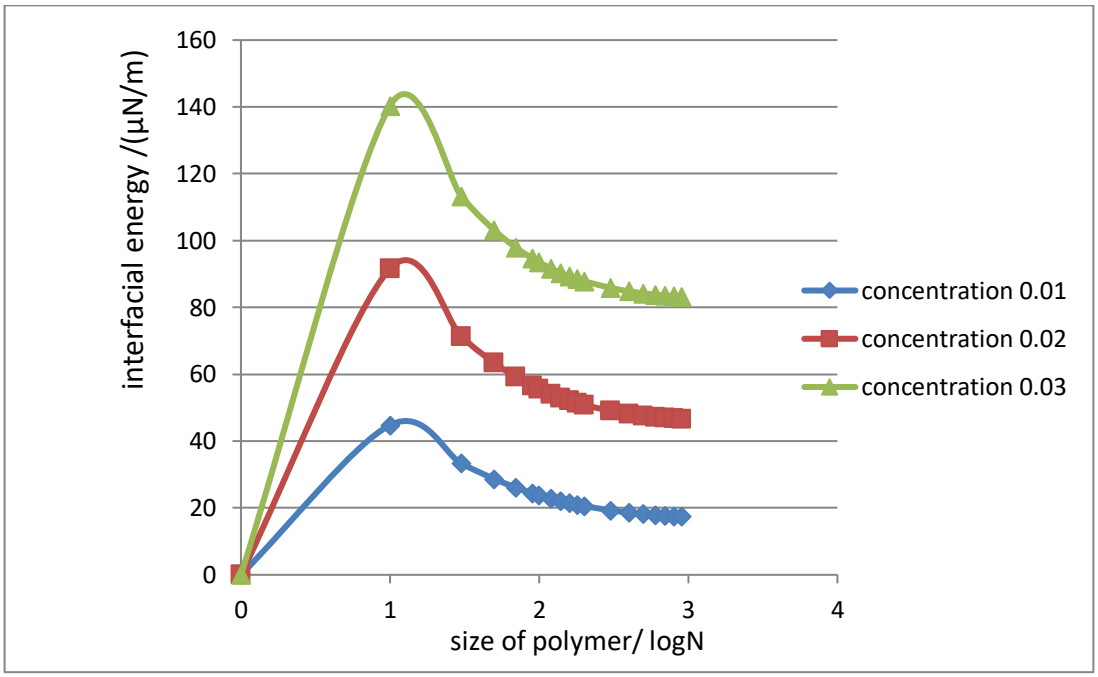

Figure 3.1.2 Interfacial energy changes with increasing sizes of polymers, plotted for different polymer concentrations.

The data of interfacial energy of the system varying from size of polymers and concentration of polymer solution has been analysed as shown in the Figure 3.1.2. It's obvious that interfacial energy reaches a peak when the monomer number is close to 10 or slightly larger than 10. Meanwhile, from data selected with different polymer volume fractions of 0.01, 0.02, 0.03, it turns out that in polymer solution with larger concentration of polymer, the interfacial energy will be significantly higher. It suggests that when concentration is 0.01, and the polymer is composed of around 10 monomers or slightly larger than 10 monomers, the energy cost of creating a solid surface, in contact with the solution is the highest. The free energy cost of creating a surface is a function of both number of excluded chains in the depletion zone and the thickness of the zone. Meanwhile, the thickness of the depletion zone depends on the

radius of gyration (and hence size) of the polymers in dilute systems (Mao, Y. et al., 1995). The former decreases with the size of the chains, if the total polymer volume fraction is kept the same, while the latter, i.e. the radius of gyration, increases with the size of the chains. A repulsive barrier exists in polymers in dilute system and the depletion potential between two spheres is related by the Boltzmann distribution to the radial distribution function of the dilute spheres (Mao, Y. et al., 1995). These two opposing effects are what leads to a peak in the interfacial energy at the same intermediate polymer chain length.

Our calculated results, shown in the above two diagrams, showed that the depletion of polymers around a surface is associated with increased free energy which means that, in absence of any specific adsorption of polymer to the surface, the contact between polymer solution and solid surface is not favoured. Indeed any disturbance that leads to a non-uniform distribution of the polymer chains will eventually involve an increase in the free energy. But we also notice that this interfacial free energy is lower for larger polymer chains than smaller ones (once we are above 10 monomers or so). Subsequently in a phase separated solution, the phase with the larger polymer chains will be the one favoured by particles, when compared to the one with smaller ones.

3.2 Partition of unequal-sized polymers in phase-separated solutions

3.2.1 The case of changing χ

In the first place, to discuss and understand the influence of changing the degree of incompatibility between two polymers, at various sizes, on partitioning effect, we choose two kinds of linear polymers chains consisting of 70 monomers and 1200 monomers, in which polymer 1 has the smaller size

of 70 monomers while polymer 2 has the larger size of 1200 monomers. The other important influencing factor, initial volume fraction, is considered to be fixed at 0.05 for each polymer, which is not uncommon commonly in real experiments utilizing biopolymer polysaccharides (Nicolai and Murray, 2017). Through plenty of tests on computer simulation program, the minimum value of interaction parameter χ where phase separation occurs has been found as 0.112 (k_bT). Below the value the two sets of chains are sufficiently compatible not to phase separate. Trying to increase χ in steps of every 0.02, from 0.13 to 0.27, the partition result of polymer volume fractions in the two phases is plotted in Figure 3.2.1.1. and Figure 3.2.1.2. Overall, Phase A contains mostly polymer 1, the smaller polymer, and very few of polymer 2. In the contrast, phase B is dominated by polymer 2, the larger polymer, and relatively few of polymer 1. As the χ increases, the degree of incompatibility is elevated, the minority polymers gradually disappear in each phase such that each phase is going to contain almost only one type of polymer, as predicted. Meanwhile, the proportion of two phases are going to become close to 0.5 as shown in Figure 3.2.1.2.

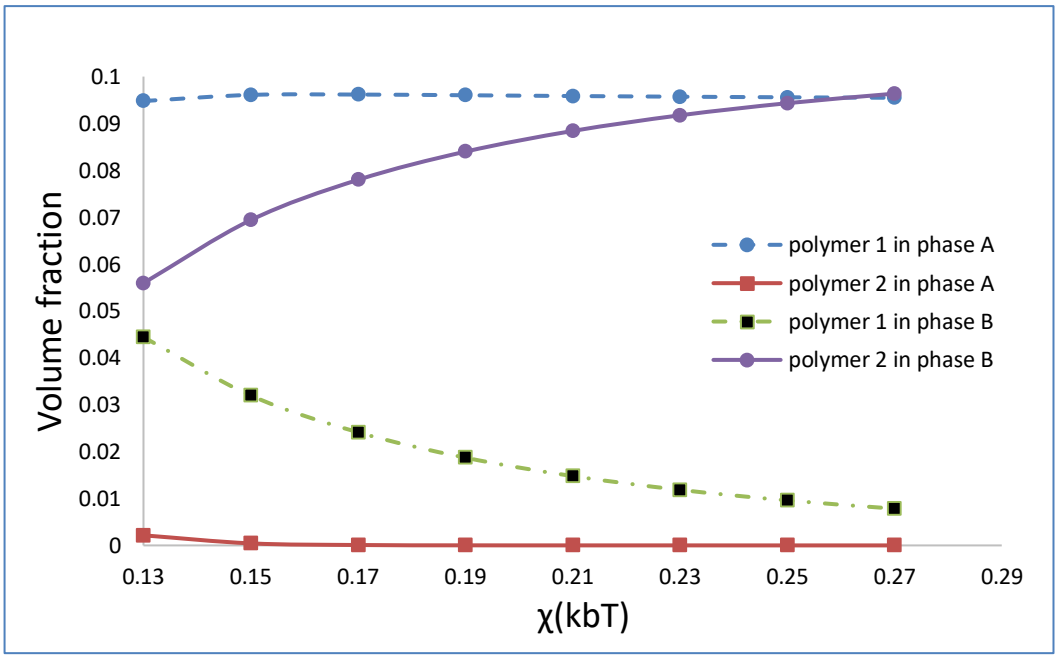

Figure 3.2.1.1 Change in the volume fraction of each type of polymer in each of the separated phase, with increasing χ .

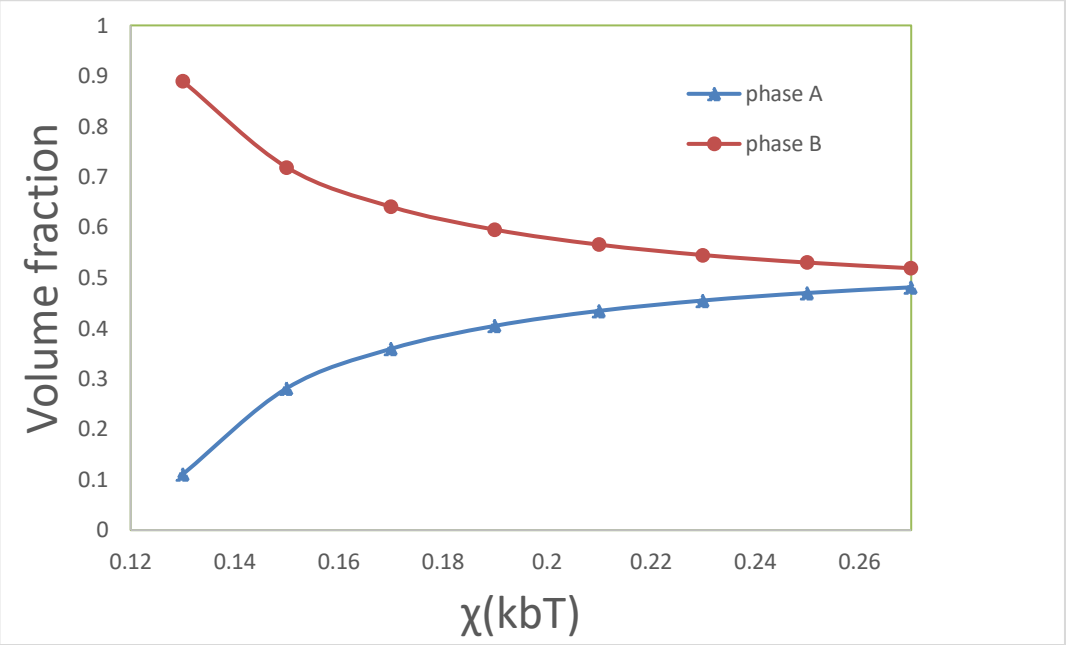

Figure 3.2.1.2 Volume fraction of the two phases in a phase separated solution, plotted as a function of the incompatibility parameter χ.

Furthermore, the interfacial energy changes of phase A and phase B against increasing χ are calculated by SCF calculations after introduction of a solid surface in each phase and results are plotted in Figure 3.2.1.3. Apparently, the free energy per unit area of phase A, plotted as solid blue line, decreases with increasing χ parameter, while the interfacial energy of phase B, plotted as dotted red line, increases. These two lines represent very similar values but have a slight difference since the interfacial energy of phase B seems to show more change than the one of phase A. This phenomenon is believed to be caused by the variation of molecular weights of two polymers and the various amount of residue free polymer molecules beyond the depletion region. Roughly, it seems that the difference between interfacial tension of phase A and phase B are gradually increasing reaching a constant value of 7.59 $\mu N m^{-1}$ for large χ (high incompatibility). The increase of difference between interfacial tension slows down though the degree of compatibility of two phases is still increasing in the same way. This phenomenon can be related to the principle of influence by χ on interfacial tension. As shown in Figure 3.2.1.1, χ impacts the composition of each phase. Meanwhile, the change of interaction parameter influences the distribution of polymers in

depletion zone as well, due to the change in the strength of interactions among polymer monomers making up the chains. Nevertheless, when χ becomes larger to promote the segregation of the polymers and they preferentially go to different phases, such interactions between polymers decreases due to the smaller level of contact between the two types of polymers, resulting to gradually constant interfacial tension for each phase. Note that changes in χ between the two polymer species do not influence the solid-solution interactions. As the consequence, the χ has a limit impact on difference between interfacial tensions of two phases, once it becomes large.

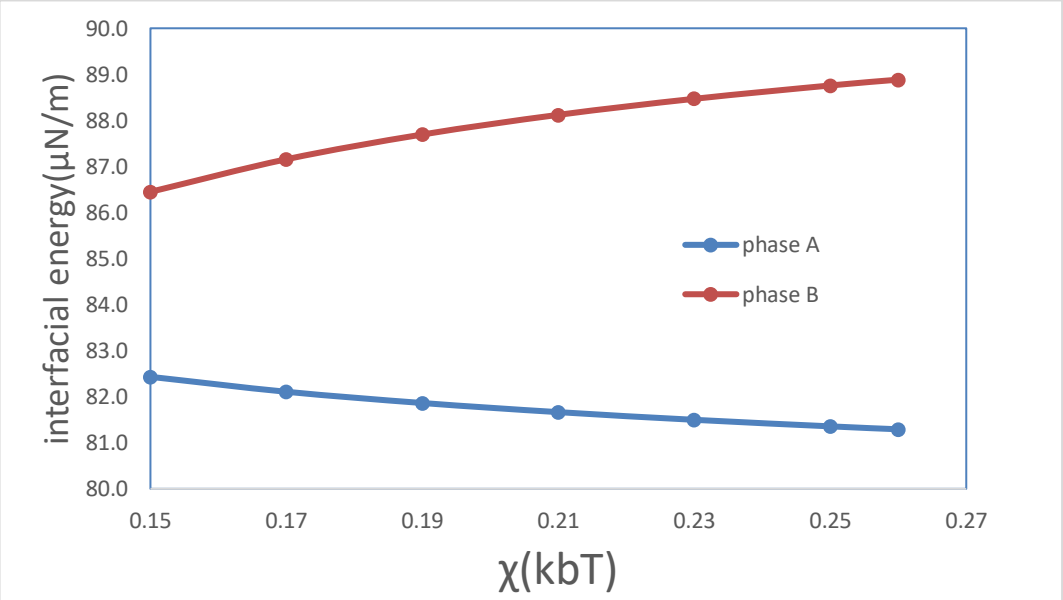

Figure 3.2.1.3 The changes of interfacial energy of each of the two phases and a solid surface with increasing χ in system as Figure 3.2.1.1.

3.2.2 The case of changing initial volume fractions of polymers

In this case, the same two polymers with degrees of polymerization of 70 and 1200 respectively, are chosen to build the solution system. Nonetheless, the changing factor is initial volume fractions of two polymers this time round. The total concentration of both polymers together is fixed at 10% in solution. On this basis, we change the proportion of two polymers from 0.04: 0.06 to 0.09:

0.01 (0.01:0.09 to 0.03:0.07 are found not to phase-separated). In addition, the important influencing factor χ is also fixed this time at 0.15. The partition result is plotted in Figure 3.2.2.1. It indicates a simple trend for all four lines, amongst which contents of polymer 1 and polymer 2 in phase A both rise linearly. Polymer 1 is dominate in the phase A, while polymer 2 takes up majority of the phase B as the initial volume fraction of polymer 1 increases. Apparently each phase is enriched with one type polymer, respectively. One interesting point observed in Figure 3.2.2.2. is that the volume fraction of phase A is apparently positively correlated to the initial overall volume fraction of polymer 1, which possesses the smaller size of the two polymers. Furthermore, volume fractions of two phases equals to each other when the initial fraction of polymer 1 reaches around 0.65, where the initial volume fraction of polymer 2 is of course 0.35.

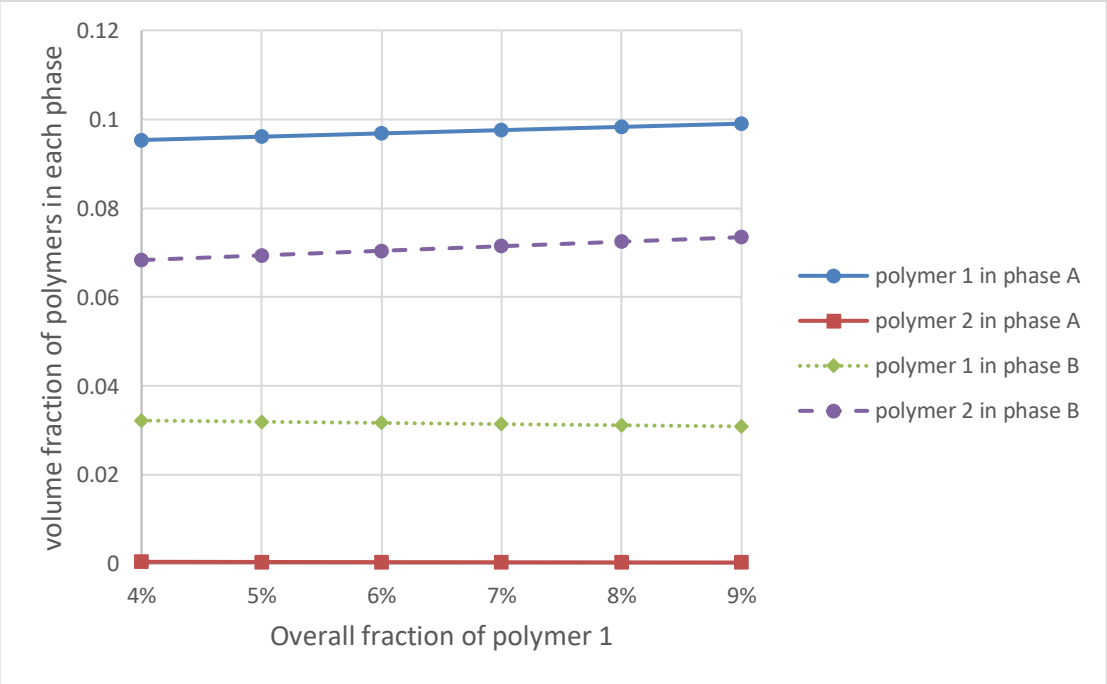

Figure 3.2.2.1 The change of volume fractions of two polymers in phase A and phase B against the increasing proportion of polymer 1 in solution, keeping the initial total volume fraction of polymers constant at the value of 10%.

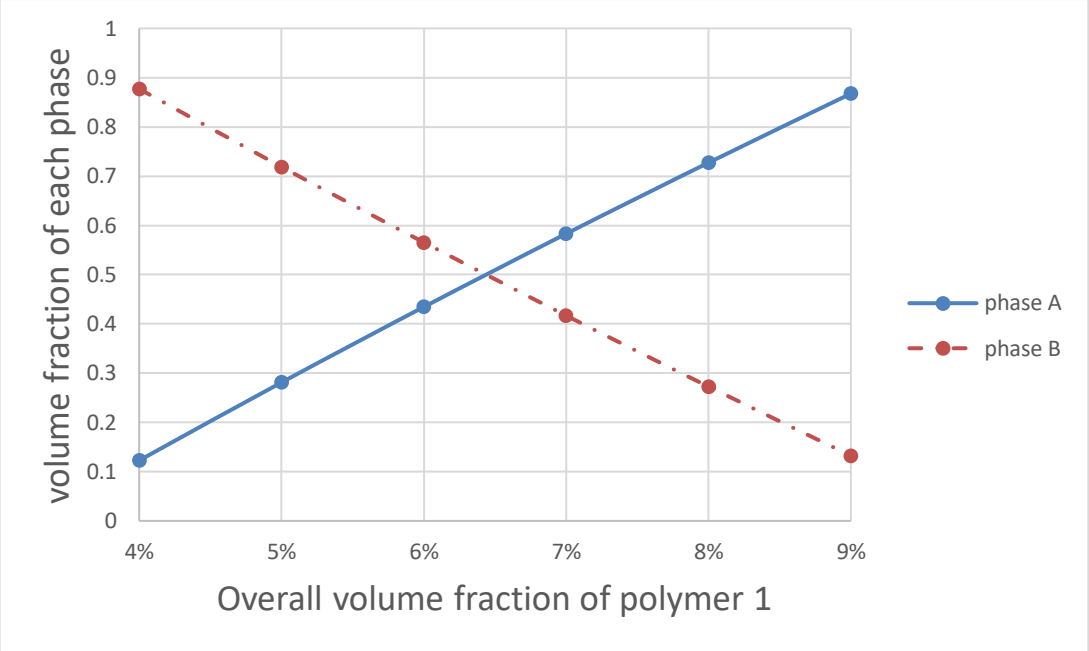

Figure 3.2.2.2 The change of volume fractions of two phases plotted against the increasing total proportion of polymer 1 in the phase-separated solution, keeping the initial total volume fraction of two polymer together constant at the value of 10%.

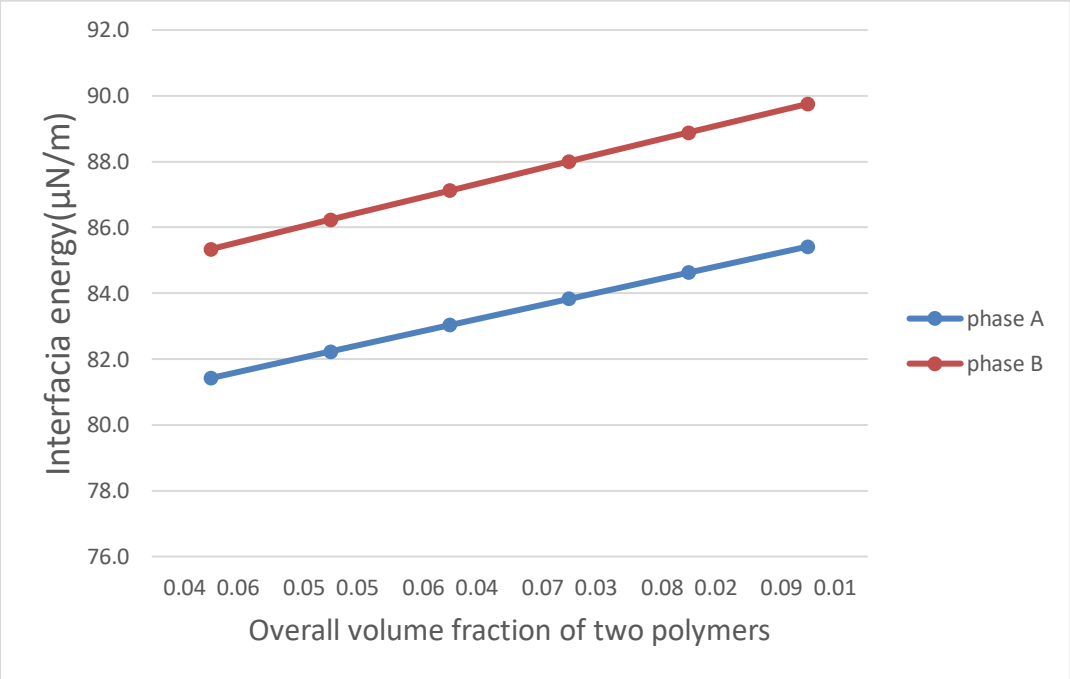

Figure 3.2.2.3 The change of interfacial energy of the two co-existing phases with a solid surface plotted against the changing initial volume fraction of two polymers.

Then the interfacial energy of these two phases are calculated as well to understand the relationship between initial volume fractions of each polymer in the solution and the resulting free energy per unit area. The result is displayed in Figure 3.2.2.3. Not surprisingly, the interfacial energy of two separated phases both increase with the higher initial volume fraction of polymer 1, both showing similar trends. However, phase B always possesses the higher free energy than phase A, though the volume fraction of phase B, as proportion of the total system constantly decreases, as seen in Figure 3.2.2.2.

In both two cases changing χ and overall volume fraction proportion, the one important common feature is one of the two separated-phases has a higher interfacial energy, and this phase retains this higher value both with increasing degree of compatibility and initial volume fraction of the smaller polymers. In comparison, the degree of compatibility χ has a stronger impact on change of partition of polymers and the interfacial energy difference between the two phases.

3.3 Prediction of fractionation of introduced particles between the two phases

As mentioned above in chapter 2, the distribution of introduced particles between the two separated phases can be predicted theoretically by equation (2.5). This can be stated more specifically with the aid of the following equation

$$\frac{n_B}{n_A} = exp\left\{\frac{-4\pi R^2(\gamma_{sB} - \gamma_{sA})}{k_B T}\right\} \qquad (3.3)$$

The left side of the equation indicates the ratio of the concentrations of the added particles in phase B relative to phase A at the final stage when equilibrium has been achieved. In right-hand side of the equation, the free

energies of each phase in phase-separated solution is multiplied by the particle surface area, which is regarded as a spherical solid substance, and are given as $4\pi R^2\gamma_{sB}$ and $4\pi R^2\gamma_{sA}$. In addition, k_B is the Boltzmann constant and T is temperature in degrees Kelvin. According to the above equation, the main influencing factors that can directly change proportion of concentrations of the added particles in the two phases and the radius of added particles, and the difference between interfacial energies of two phases. The difference between interfacial energies of two phases were shown in Figure 3.2.1.3. and Figure 3.2.2.3. In the case of changing χ of unequal-sized polymer solution, the phase separation occurs above $\chi > 0.112$, and the difference of interfacial energies of two phases gradually approached a constant value as χ increased. We can take $\chi = 0.15$ as an example, where the corresponding interfacial energy difference $(\gamma_{sB} - \gamma_{sA})$ is 4.02 μN/m, again as seen in Figure 3.2.1.3. When the radius of the particle is set at 0.5 μm, the result for $\frac{n_B}{n_A}$ is obtained to be $e^{(-3071)}$, which is negligible. Therefore, in this situation with minimum $(\gamma_{sB} - \gamma_{sA})$, particles prefer to segregate almost completely into phase A, which is richer in smaller polymers. As shown in Figure 3.2.1.3, the difference of interfacial energies of two phases keeps increasing and then gradually become stable at 7.59 μN/m. It is clear that the value of $\frac{n_B}{n_A}$ would become even smaller with further increasing $(\gamma_{sB} - \gamma_{sA})$ occurring due to the higher degree in compatibility between the two sets of polymers. Consequently, almost all the introduced particles in this system are going to reside in phase A, irrespective of how they are introduced into the system, once equilibrium is attained. As for the second case of increasing initial volume fraction of polymer 1, a similar conclusion is arrived at. It has been known that the difference of interfacial energies between two phases approaches a constant of 4.33 μN/m, which leads to the value of $\frac{n_B}{n_A}$ be $e^{(-3308)}$. Again, this is very small and the added particles tend to go almost completely to phase A, irrespective of further increase in the overall volume fraction proportion of polymer 1. This prediction matches the experimental results reported that particles significantly prefer to reside to one certain phase region and not the other. Various measures had

to be taken to eliminate the influence of affinity between polymers and solid surface of particles (Moschakis et al., 2018) to ensure that the particles is inert with respect to adsorption of both groups of polymers on its surface. However, when the radius become very small, say at 1 nm and with $\chi = 0.15$, the $\frac{n_B}{n_A} \approx 1$. Thus, it can be seen that radius of particles influences the partition of particles in each phase quite significantly, leading to the possibility to apply this theoretical prediction as a way to separate and extract different sized particles from a polydispersed dispersion of such particles in the future.

3.4 The situation of particles trapped in two phases

In section 1.4, it has been discussed that when particles are attached to the interface, the required detachment energy is mainly related to the radius of spherical particles, the interfacial tension and the contact angle θ. The contact angle θ actually describes the situation of particles penetrating the interface between two phases. It can be illustrated as in the following image

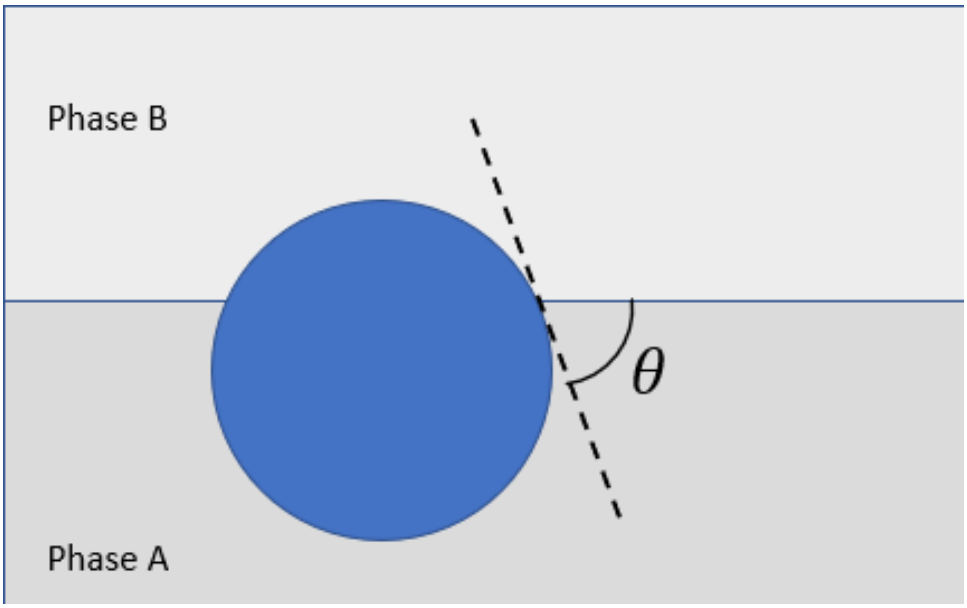

Figure 3.4 A Particle at interface between two co-existing phases where the contact angle θ has been illustrated.

As the Figure 3.4 shows, the particle is located right at the interface between the two phases and it penetrates both phases with various degree. Basically, the interface between the two phases is assumed to be much thinner than the size of added particle. The angle produced between the tangent line and the interface is recognized as the contact angle θ. Normally the contact angle, by definition, is measured into the denser phase. It can be shown that Young's equation,

$$\cos(\theta) = \frac{(\gamma_{sB} - \gamma_{sA})}{\gamma_{AB}} \qquad (3.4.1)$$

where γ_{AB} is the interfacial tension of the interface between phase A and phase B. This equation is known as Young's equation. The value of γ_{AB} has been deduced and measured in many relevant work to be in the range 1 to 100 $\mu N m^{-1}$or even slightly lower, changing with the nature of the polymer species and their concentrations (Scholten et al., 2006b; Scholten et al., 2006a) (Balakrishnan et al., 2012). Young's equation implies that when the introduced particle is located at the interface if is not equally wetted by the two phases, the value of $|\cos(\theta)|$ should be always be below 1. Therefore, it requires $|\gamma_{sB} - \gamma_{sA}| < \gamma_{AB}$ to make sense. If $|\gamma_{sB} - \gamma_{sA}| > \gamma_{AB}$, then particle will not set on interface and will be fully wetted by one of the phases. Fortunately, this requirement is not so difficult to satisfy in practical, the value of $\gamma_{sB} - \gamma_{sA}$ is commonly below 10 $\mu N m^{-1}$, and sometime even lower than 1 $\mu N m^{-1}$. One thing should be noticed that two types of polymers both shows no specific stronger affinity to solid surface of particles as compared to the other species.

Regarding γ_{AB}, it has been discussed in the study by (Broseta, 1987) (Ettelaie et al., 2019). Here we give a brief explanation. Firstly, it can be derived by the following equation deduced by Helfand and Tagami (1972) using self-consistent field theory in the context of Cahn-Hilliard approximation. This leads to the following equation.

$$\gamma_{AB} = \left(\frac{k_B T}{{a_0}^2}\right) / \sqrt{\frac{\chi}{6}} \qquad (3.4.2)$$

According to the above equation, the γ_{AB} is clearly related mainly to the interaction parameter χ. However, it was derived for two immiscible polymer melts, whilst the present study aims at the immiscible polymer solutions. For two polymer solutions, the corresponding description for γ_{AB} is shown to be as following (De Gennes, 1979) (Broseta et al., 1987)

$$\gamma_{AB} = \phi^{1.65} \left(\frac{k_B T}{{a_0}^2}\right) / \sqrt{\frac{\chi}{6}} \qquad (3.4.3)$$

Thus, applying the above equation to calculate the contact angle θ, it turns out that $\cos(\theta) \sim \chi^{-1/2}$, when χ.becomes very large. As the interfacial energy difference between two phases reaches a constant value. This combination with the fact that $\gamma_{AB} \sim \chi^{1/2}$ can be used to arrive at the result for the contact angle. And in turn, when the interaction parameter infinitely increases, $\gamma_{AB} \sim \chi^{1/2}$, so γ_{AB} becomes extremely large and the contact angle correspondingly decreases as $\cos(\theta) \approx 0$. Therefore, the contact angle produced between particle surface and the interface between two phases is going to be 90° with the increase of degree of incompatibility. The description of γ_{AB} for more cases is discussed and improved by (Broseta et al., 1987) and (Tromp, R. and Blokhuis, 2013). In practical, the distribution of components at interface is complicated, aggregation of solvent molecules would affect the contact between two types of polymers. As for the present study, since χ ranges from 0.15 to 0.26, the γ_{AB} is calculated to be from 36.4~63.2 $\mu N/m$. Meanwhile, the difference between interfacial tensions of two phases $\gamma_{sB} - \gamma_{sA}$ is approaching 7.59 $\mu N/m$, leading to the contact angle calculated to approach 83.1°. As the χ increases, the contact angle is approaching to 90° consequently.

3.5 The phase separation determination

The mixtures of κ-carrageenan and konjac gum were observed to determine the phase separation phenomenon after being placed overnight in the cupboard at the room temperature. Phase separation occurs in various concentration groups. In phase-separated solutions, there are two phases co-existing in the tubes, amongst which the upper one looks clearer and more transparent, and the lower one seems to be very sticky and dense. To give an example, the light microscopy images, for 0.9 wt% κ-carrageenan solution and 0.9 wt% konjac gum solution are shown as Figure 3.5.1. In addition, in the phase-separated solution mixed by these two polysaccharide solutions, the microscopy images for the upper phase and lower phase are shown in Figure 3.5.2. Comparing the light microscopy images got for each solution before their mixing, as in Figure 3.5.1, to images observed for upper and lower phases (Figure 3.5.2). It can be seen that the upper phase in the tube is the phase enriched with κ-carrageenan, while the lower phase is the phase richer in konjac gum.

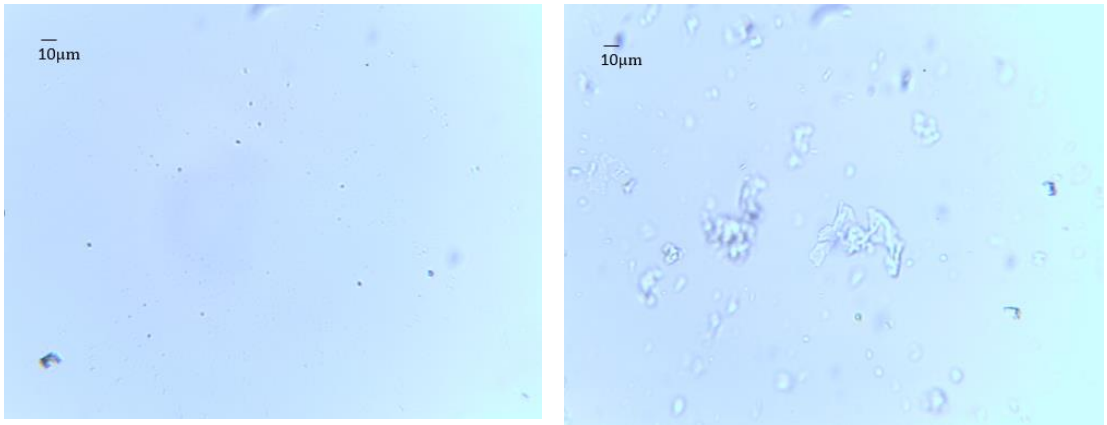

Figure 3.5.1 0.9 wt% κ-carrageenan solution, 0.9 wt% konjac gum solution.

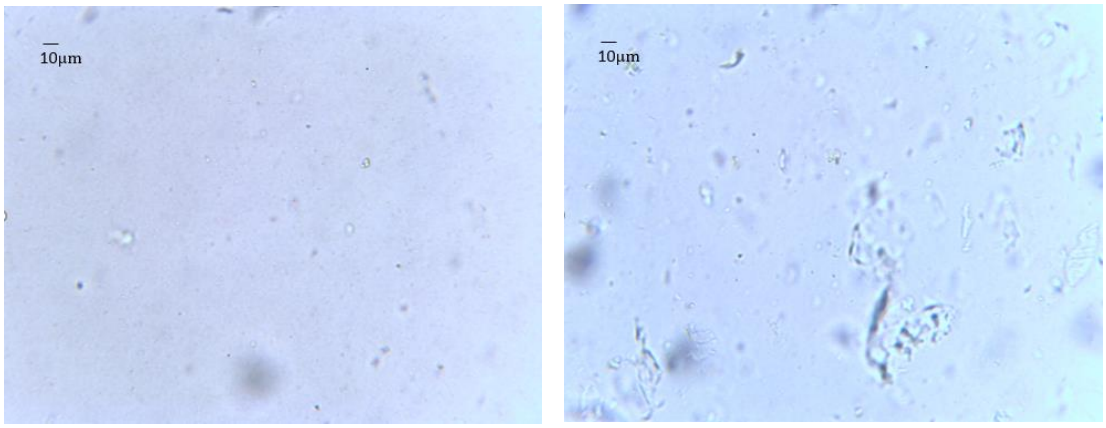

Figure 3.5.2. The upper phase in the mixture, the lower phase in mixture following phase separation.

As declared in chapter 2 Methodology, mixtures are composed of various concentrations of two polysaccharide solutions: blending 0.1 wt% to 1.0 wt% -carrageenan solution and 0.1 wt% to 1.0 wt% konjac gum solution respectively, and observe the mixtures after one day past mixing, the phase diagram has been drawn as in Figure 3.5.3.

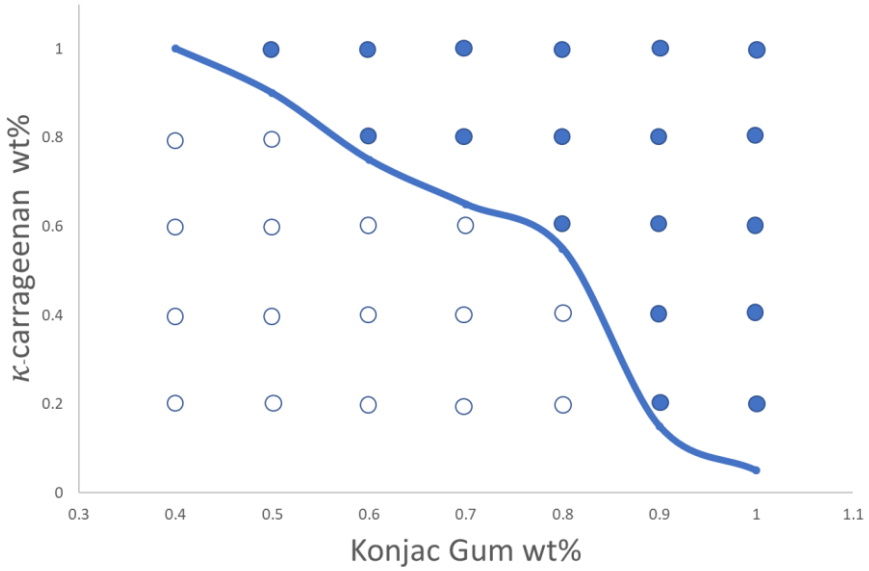

Figure 3.5.3 Phase diagram demonstrating the stable and phase separated regions. The coloured round dots are for phase-separated solutions, white dots are solutions remaining monogenous single phase, the solid line is the phase boundary.

In the above diagram, the coloured round dots represent the mixture comprising of two coexisting phases, white dots represent the composition that do not phase-separate and remain as a single homogenous solution. It shows a tendency that the combination of two polysaccharides solutions with higher concentrations are more prone to phase saparation. The plot area is divided by a trendline, above which is the region where phase separation occurs. For the konjac gum at low concentrations, from 0.1 wt% to 0.5 wt%, only when mixed with 1.0 wt% κ-carrageenan solution any phase separation can occur. As the concentration of konjac gum in the solution is increased, the lowest concentration of κ-carrageenan to induce phase separation is seen to decrease. It is obvious that the phase boundary drops dramatically when konjac gum solution reaches 0.9 wt%. Especially for 1.0 wt% konjac gum, phase separation occurs even when there is only 0.1 wt% κ-carrageenan in the mixed solution. Similarly, but not exactly the same, a 0.9 wt% of κ-carrageenan or higher can be blended with as low as 0.1 wt% konjac gum to cause phase separation. As was discussed in Chapter 1, the possible situations for phase separation are illustrated in Figure 1.2.1 demonstrating that the biopolymers concentrations ought to be high enough for there to be an incentive for the phase separation.

3.6 Fluorescent particle preference in two phases

The introduction of fluorescent particles, Carboxyl-modified polystyrene P(S/V-COOH), was implemented to observe whether the introduced particles would preferentially reside in one of the two separated phases. These particles were added with a concentration of 0.2 vol.% into the konjac gum solution first, and then we add the same volume of κ-carrageenan solution into the tube to blend the two biopolymer solutions together. After the heating for 1hr and long-time storage, phase separation occurs. Meanwhile, the particles distribution situations in two phases shows difference and the confocal microscopy was used to clarify the distribution of fluorescent particles in the two separated phases. Comparing Figure 3.6.1. and 3.6.2., which are confocal microscopy images for upper and lower phases, respectively, it is

clear that the upper phase contains substantially more fluorescent particles than the lower phase. In other words, fluorescent particles tend to reside into the phase enriched with κ-carrageenan, rather than the phase richer in konjac gum. To verify no specific electrostatic affinity between fluorescent particles and there two types of polymers, the pH of the two polymer solutions and two phases after phase separation, as well as zeta potential of the fluorescent particles are measured and the result presented in Table 3.6. Zeta potential describes the potential difference between the dispersion medium and the surrounding layer of fluid attached to the dispersed particles.

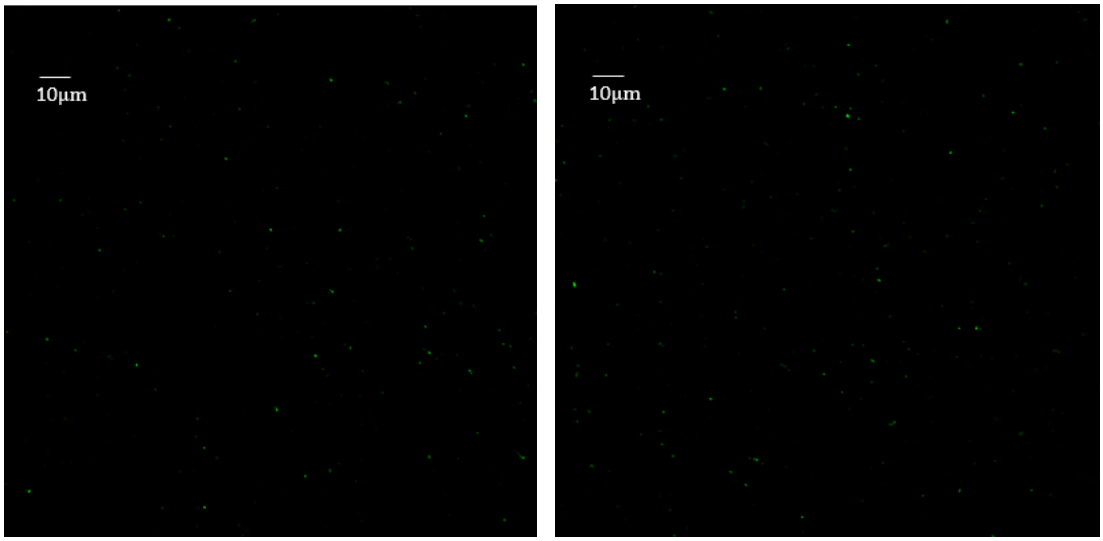

Figure 3.6.1 Confocal microscopy images for the upper phase. The light green dots are fluorescent particles. The average number of these is counted to be 45 in these micrographs.

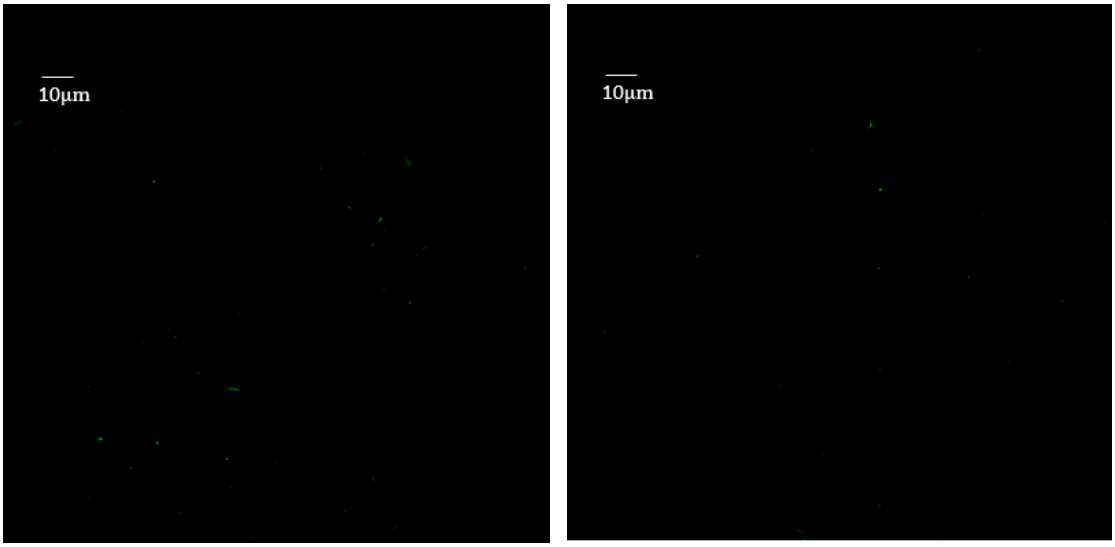

Figure 3.6.2 Confocal microscopy images for the lower phase. The light green dots are fluorescent particles. The average number of these is counted to be 13 in the micrograph.

	κ – carrageenan solution	Konjac gum solution	The upper phase	The lower phase	Fluorescent particles
pH	6.79	5.20	6.35	6.27	
Zeta potential					-31.7 mV

Table 3.6 pH values of two solutions and two phases in phase separated solution, zeta potential of the fluorescent particles dispersing in water.

In the present study, the zeta potential of the fluorescent particles measured by zetasizer indicates that the particles are apparently negative, whilst two polysaccharides solution and two phases in phase separated solution are neutral or slightly negative. The results prove that there's no electrostatic preference between particles and either type of polymers. Combined with confocal images above, the similar conclusion can be obtained that introduced

non-adsorbed particles tend to aggregate into the phase enriched with smaller polymers in phase separated solution.

Chapter 4
Conclusion

In this work, the principle of phase separation in solutions containing two incompatible polymers is introduced and furthermore the phase separation results and the corresponding interfacial tension are simulated and calculated by computer program applying SCF calculations. Prediction of tendency of inert particles into the phase enriched with polymers of smaller polymer size (kDa) in two polymers has been approved. The incentive for the phenomenon is the preference to region with lower entropy and higher stability in polymer solution system. The particles overwhelmingly partition into the solution phase containing the smaller chains (i.e. with a degree of polymerization N=…). It turns out that while both sets of polymers do not have any tendency to adsorb on the surface of particles, they do avoid the region around the particle surface. Reason for this is that polymers close to the interface will lose some degree of configurational entropy (i.e. are more restricted than in bulk) since they cannot penetrate into the solid particles. Associated with the formation of this polymer depleted interface between the solid surface and both of the two separated solution phases. It turns out that this free energy per unit surface area (i.e. solid-solution interfacial tension) is slightly lower for the solution phase with the smaller chains. The difference is only ~ 1 micro N/m as found in this project. While this seems very small, the total energy $4\pi R^2 \Delta\gamma$ is hundreds of kbT. This is more than enough then to force the particles to partition almost completely into the phase with smaller polymer chains. We also explored and discussed the influence of degree of incompatibility and degree of polymerization, initial proportion of volume fraction of polymers. For two cases of changing χ and initial proportion of volume fraction of polymers, the interfacial tension is always approaching a constant value when the influencing factor increases. The contact angle produced between trapped introduced particles and the interface between two phases is close to 90° with the sufficiently large χ.

Experimental work has been done to assist verify the tendency of fluorescent particles in two phases enriched with incompatible polysaccharides. It turns

out to be in accord with the theoretical prediction. In the precondition of no specific affinity between fluorescent particles and two polysaccharides, the fluorescent particles preferentially accumulate into the upper phase enriched with κ−carrageenan, which is the smaller polysaccharide in two biopolymers.

Bibliography

Al‐Ghazzewi, F.H., Khanna, S., Tester, R.F. and Piggott, J. 2007. The potential use of hydrolysed konjac glucomannan as a prebiotic. *Journal of the Science of Food and Agriculture.* **87**(9), pp.1758-1766.

Alves, M., Antonov, Y.A. and Gonçalves, M. 1999. The effect of structural features of gelatin on its thermodynamic compatibility with locust bean gum in aqueous media. *Food Hydrocolloids.* **13**(2), pp.157-166.

Balakrishnan, G., Nicolai, T., Benyahia, L. and Durand, D. 2012. Particles trapped at the droplet interface in water-in-water emulsions. *Langmuir.* **28**(14), pp.5921-5926.

Bohmer, M.R., Evers, O.A. and Scheutjens, J.M. 1990. Weak polyelectrolytes between two surfaces: adsorption and stabilization. *Macromolecules.* **23**(8), pp.2288-2301.

Broseta, D., Leibler, L., Ould Kaddour, L. and Strazielle, C. 1987. A theoretical and experimental study of interfacial tension of immiscible polymer blends in solution. *The Journal of chemical physics.* **87**(12), pp.7248-7256.

Chun, J.-Y., Hong, G.-P., Surassmo, S., Weiss, J., Min, S.-G. and Choi, M.-J. 2014. Study of the phase separation behaviour of native or preheated WPI with polysaccharides. *Polymer.* **55**(16), pp.4379-4384.

Chung, C., Degner, B. and McClements, D.J. 2013. Controlled biopolymer phase separation in complex food matrices containing fat droplets, starch granules, and hydrocolloids. *Food research international.* **54**(1), pp.829-836.

Daniel-da-Silva, A.L., Ferreira, L., Gil, A.M. and Trindade, T. 2011. Synthesis and swelling behavior of temperature responsive κ-carrageenan nanogels. *Journal of colloid and interface science.* **355**(2), pp.512-517.

De Gennes, P.-G. and Gennes, P.-G. 1979. *Scaling concepts in polymer physics.* Cornell university press.

Dickinson, E. 2018. Particle-based stabilization of water-in-water emulsions containing mixed biopolymers. *Trends in food science & technology.*

Dickinson, E., Horne, D., Phipps, J. and Richardson, R. 1993. A neutron reflectivity study of the adsorption of. beta.-casein at fluid interfaces. *Langmuir.* **9**(1), pp.242-248.

Ding, P., Wolf, B., Frith, W., Clark, A., Norton, I. and Pacek, A. 2002. Interfacial tension in phase-separated gelatin/dextran aqueous mixtures. *Journal of colloid and interface science.* **253**(2), pp.367-376.

Dolan, A. and Edwards, W.F. 1975. The effect of excluded volume on polymer dispersant action. *Proceedings of the Royal Society of London. A. Mathematical and Physical Sciences.* **343**(1635), pp.427-442.

Esquena, J. 2016. Water-in-water (W/W) emulsions. *Current Opinion in Colloid & Interface Science.* **25**, pp.109-119.

Ettelaie, R., Dickinson, E. and Pugnaloni, L. 2014a. First-order phase transition during displacement of amphiphilic biomacromolecules from interfaces by surfactant molecules. *Journal of Physics: Condensed Matter.* **26**(46), p464109.

Ettelaie, R., Khandelwal, N. and Wilkinson, R. 2014b. Interactions between casein layers adsorbed on hydrophobic surfaces from self consistent field theory: κ-casein versus para-κ-casein. *Food Hydrocolloids.* **34**, pp.236-246.

Ettelaie, R., Murray, B.S. and Liu, S. 2019. On the Origin of Seemingly Non-Surface Active Particles Partitioning between Phase Separated Solutions of Incompatible Non-Adsorbing Polymers and Their Adsorption at the Phase Boundary. *Langmuir.*

Firoozmand, H., Murray, B.S. and Dickinson, E. 2009. Interfacial structuring in a phase-separating mixed biopolymer solution containing colloidal particles. *Langmuir.* **25**(3), pp.1300-1305.

Fleer, G. and Scheutjens, J. 1987. Effect of adsorbing and nonadsorbing polymer on the interaction between colloidal particles. *Croatica Chemica Acta.* **60**(3), pp.477-494.

Fleer, G., Stuart, M.C., Scheutjens, J.M., Cosgrove, T. and Vincent, B. 1993. *Polymers at interfaces.* Springer Science & Business Media.

Flory, P.J. 1953. *Principles of polymer chemistry.* Cornell University Press.

Glicksman, M. 2019. *Food hydrocolloids.* Crc Press.

Grinberg, V.Y. and Tolstoguzov, V. 1997. Thermodynamic incompatibility of proteins and polysaccharides in solutions. *Food Hydrocolloids.* **11**(2), pp.145-158.

Helfand, E. and Tagami, Y. 1972. Theory of the interface between immiscible polymers. II. *The Journal of chemical physics.* **56**(7), pp.3592-3601.

Leermakers, F.A., Atkinson, P.J., Dickinson, E. and Horne, D.S. 1996. Self-consistent-field modeling of adsorbed β-casein: effects of pH and ionic strength on surface coverage and density profile. *Journal of Colloid and Interface Science.* **178**(2), pp.681-693.

Levine, S., Bowen, B.D. and Partridge, S.J. 1989. Stabilization of emulsions by fine particles I. Partitioning of particles between continuous phase and oil/water interface. *Colloids and surfaces.* **38**(2), pp.325-343.

Majzoobi, M., Talebanfar, S., Eskandari, M.H. and Farahnaky, A. 2017. Improving the quality of meat‐free sausages using κ‐carrageenan, konjac mannan and xanthan gum. *International Journal of Food Science & Technology.* **52**(5), pp.1269-1275.

Mao, Y., Cates, M. and Lekkerkerker, H. 1995. Depletion force in colloidal systems. *Physica A: Statistical Mechanics and its Applications.* **222**(1-4), pp.10-24.

Matalanis, A., Jones, O.G. and McClements, D.J. 2011. Structured biopolymer-based delivery systems for encapsulation, protection, and release of lipophilic compounds. *Food Hydrocolloids.* **25**(8), pp.1865-1880.

Morris, E.R., Rees, D.A. and Robinson, G. 1980. Cation-specific aggregation of carrageenan helices: domain model of polymer gel structure. *Journal of molecular biology.* **138**(2), pp.349-362.

Moschakis, T., Chantzos, N., Biliaderis, C.G. and Dickinson, E. 2018. Microrheology and microstructure of water-in-water emulsions containing sodium caseinate and locust bean gum. *Food & function.* **9**(5), pp.2840-2852.

Moschakis, T., Murray, B.S. and Dickinson, E. 2006. Particle tracking using confocal microscopy to probe the microrheology in a phase-separating emulsion containing nonadsorbing polysaccharide. *Langmuir.* **22**(10), pp.4710-4719.

Murray, B.S. and Phisarnchananan, N. 2014. The effect of nanoparticles on the phase separation of waxy corn starch+ locust bean gum or guar gum. *Food Hydrocolloids.* **42**, pp.92-99.

Nicolai, T. and Murray, B. 2017. Particle stabilized water in water emulsions. *Food Hydrocolloids.* **68**, pp.157-163.

Norton, I. and Frith, W. 2001. Microstructure design in mixed biopolymer composites. *Food Hydrocolloids.* **15**(4-6), pp.543-553.
Pai, V., Srinivasarao, M. and Khan, S.A. 2002. Evolution of microstructure and rheology in mixed polysaccharide systems. *Macromolecules.* **35**(5), pp.1699-1707.
Peddireddy, K.R., Nicolai, T., Benyahia, L. and Capron, I. 2016. Stabilization of water-in-water emulsions by nanorods. *ACS Macro Letters.* **5**(3), pp.283-286.
Piculell, L. and Lindman, B. 1992. Association and segregation in aqueous polymer/polymer, polymer/surfactant, and surfactant/surfactant mixtures: similarities and differences. *Advances in Colloid and Interface Science.* **41**, pp.149-178.
Poortinga, A.T. 2008. Microcapsules from self-assembled colloidal particles using aqueous phase-separated polymer solutions. *Langmuir.* **24**(5), pp.1644-1647.
Pryamitsyn, V.A., Leermakers, F., Fleer, G. and Zhulina, E. 1996. Theory of the collapse of the polyelectrolyte brush. *Macromolecules.* **29**(25), pp.8260-8270.
Sagis, L.M. 2008. Dynamics of controlled release systems based on water-in-water emulsions: a general theory. *Journal of Controlled Release.* **131**(1), pp.5-13.
Scheutjens, J. and Fleer, G. 1979. Statistical theory of the adsorption of interacting chain molecules. 1. Partition function, segment density distribution, and adsorption isotherms. *Journal of Physical Chemistry.* **83**(12), pp.1619-1635.
Scheutjens, J. and Fleer, G. 1980. Statistical theory of the adsorption of interacting chain molecules. 2. Train, loop, and tail size distribution. *The Journal of Physical Chemistry.* **84**(2), pp.178-190.
Scholten, E., Sagis, L.M. and van der Linden, E. 2006a. Effect of bending rigidity and interfacial permeability on the dynamical behavior of water-in-water emulsions. *The Journal of Physical Chemistry B.* **110**(7), pp.3250-3256.
Scholten, E., Sprakel, J., Sagis, L.M. and van der Linden, E. 2006b. Effect of interfacial permeability on droplet relaxation in biopolymer-based water-in-water emulsions. *Biomacromolecules.* **7**(1), pp.339-346.
Stratford, K., Adhikari, R., Pagonabarraga, I., Desplat, J.-C. and Cates, M.E. 2005. Colloidal jamming at interfaces: A route to fluid-bicontinuous gels. *Science.* **309**(5744), pp.2198-2201.
Takigami, S. 2009. Konjac mannan. *Handbook of hydrocolloids.* Elsevier, pp.889-901.
Tromp, R. and Blokhuis, E. 2013. Tension, rigidity, and preferential curvature of interfaces between coexisting polymer solutions. *Macromolecules.* **46**(9), pp.3639-3647.
Tromp, R.H., Tuinier, R. and Vis, M. 2016. Polyelectrolytes adsorbed at water–water interfaces. *Physical Chemistry Chemical Physics.* **18**(45), pp.30931-30939.
Van der Sman, R. and Meinders, M. 2011. Prediction of the state diagram of starch water mixtures using the Flory–Huggins free volume theory. *Soft Matter.* **7**(2), pp.429-442.
Yaseen, E., Herald, T., Aramouni, F. and Alavi, S. 2005. Rheological properties of selected gum solutions. *Food Research International.* **38**(2), pp.111-119.

Zembyla, M., Murray, B.S. and Sarkar, A. 2018. Water-in-oil Pickering emulsions stabilized by water-insoluble polyphenol crystals. *Langmuir.* **34**(34), pp.10001-10011.
Ziegel, E. 1987. *Numerical recipes: The art of scientific computing*. Taylor & Francis Group.